Palaeomagnetism of flood basalts in the Pilbara Craton, Western Australia: Late Archaean continental drift and the oldest known reversal of the geomagnetic field

Geert Strik,[1] Tim S. Blake,[2] Tanja E. Zegers,[1] Stan H. White,[3] and Cor G. Langereis[1]

Received 27 February 2003; revised 29 May 2003; accepted 14 July 2003; published 3 December 2003.

[1] A late Archaean (circa 2775–2715 Ma) succession of terrestrial continental flood basalts, mafic tuffs, felsic volcanic rocks, and clastic sedimentary rocks in the Nullagine Synclinorium (and Meentheena Centrocline) of the East Pilbara Basin, Western Australia, has been sampled for a palaeomagnetic study. Over 500 oriented, mostly basalt, drill cores were collected from the supracrustal succession and associated dykes. Thermal and alternating field demagnetization revealed two distinct components. Positive fold, conglomerate, and reversal tests confirm that the primary natural remanent magnetization (NRM) is still preserved. The secondary component is interpreted as the record of remagnetization during a major thermal event, possibly in the Early Proterozoic. Analysis of the primary NRM directions results in a magnetostratigraphy and an apparent polar wander path (APWP) for the 60 Myr interval covered by the sampled succession. Assuming a geocentric axial dipole during this time interval, the APWP shows that the Pilbara Craton was drifting during the late Archaean and that drift rates probably varied significantly. In particular, a mean 27.2° shift in palaeolatitude is recorded across an unconformity that represents a relatively short time period and that marks a significant change in basalt geochemistry. This study suggests that continents moved horizontally during the late Archaean and that the rates of movement were significantly faster than in the Phanerozoic. In addition, a reversed polarity interval, with a positive reversal test, is recorded. We argue that it documents the oldest known geomagnetic reversals of the geomagnetic field. *INDEX TERMS:* 1525 Geomagnetism and Paleomagnetism: Paleomagnetism applied to tectonics (regional, global); 1535 Geomagnetism and Paleomagnetism: Reversals (process, timescale, magnetostratigraphy); 8125 Tectonophysics: Evolution of the Earth; 8157 Tectonophysics: Plate motions—past (3040); 9619 Information Related to Geologic Time: Precambrian; *KEYWORDS:* paleomagnetism, Archean, Pilbara, drift rates, flood basalts, reversals

Citation: Strik, G., T. S. Blake, T. E. Zegers, S. H. White, and C. G. Langereis, Palaeomagnetism of flood basalts in the Pilbara Craton, Western Australia: Late Archaean continental drift and the oldest known reversal of the geomagnetic field, *J. Geophys. Res.*, *108*(B12), 2551, doi:10.1029/2003JB002475, 2003.

1. Introduction

[2] The nature of Archaean (4.0–2.5 Ga) tectonic processes is largely unknown and often controversial. Schools of thought still vary widely despite decades of research on all continents [e.g., *Hamilton*, 1998; *de Wit*, 1998]. Central to all controversies concerning larger-scale tectonic processes is the question to which degree Archaean continental crust moved horizontally across the Earth's surface, in other words, whether it was dominated by horizontal or vertical tectonics.

[1]Palaeomagnetic Laboratory Fort Hoofddijk, Utrecht University, Utrecht, Netherlands.
[2]Chidlow, Western Australia, Australia.
[3]Department of Earth Sciences, Utrecht University, Utrecht, Netherlands.

0148-0227/03/2003JB002475$09.00

[3] Palaeomagnetism, in conjunction with high-resolution isotopic and biostratigraphic age control, has proven crucial to quantifying both the rotation and latitudinal displacement of the Earth's plates during the Phanerozoic. However, in rocks older than circa 180 Ma the oceanic polarity record is not available, and in Precambrian rocks there is poor biostratigraphic control and commonly only widely spaced isotopic ages. In addition, Precambrian rocks are commonly deformed and metamorphosed, rendering them unsuitable for palaeomagnetic studies. Therefore with increasing age, it becomes more difficult to derive and interpret palaeomagnetic data.

[4] In Archaean rocks, palaeomagnetic studies are even more problematic because there is an even greater paucity of well-exposed, unaltered, and undeformed rocks that are suitable for palaeomagnetic studies. Further, Archaean tectonic processes are still poorly understood, which makes interpreting the meaning of any palaeomagnetic results problematic. While there is a broad consensus that the

Archaean mantle was substantially hotter than today [e.g., *Pollack*, 1997], there is little consensus concerning larger-scale tectonic processes. For example, *Hamilton* [1998] argues that plate tectonic processes such as those evoked for the Phanerozoic did not occur until at least 2.6 Ga and concludes that no observational evidence for rifting, rotation, and continental plate reassembly has been found to support plate tectonic activity. In contrast, *de Wit* [1998] argues that the evidence for plate tectonics in the late Archaean is strong and that the process appears to dominate this time period.

[5] Palaeomagnetic studies can make a significant contribution to this debate, provided they have sufficient geological and geochronological control and provided that they demonstrate a primary natural remanent magnetization (NRM). However, little is known about the Archaean geomagnetic field, and certain assumptions have to be made when interpreting Archaean NRM. In particular, we have to assume that the Earth's magnetic field behaved as a geocentric axial dipole (GAD), even though it is still a topic of debate. For example, *Kent and Smethurst* [1998] conclude that a 25% octupole contribution to the axial dipole field can explain the anomalous inclination distribution for the Precambrian and Palaeozoic, based on the bias toward low inclinations of known data from the Global Palaeomagnetic Database (GPMDB). However, *McElhinny and McFadden* [2000] claim that it is more probable that continental lithosphere had the tendency to be cycled into the equatorial belt and that the database used by *Kent and Smethurst* [1998] does not allow a sufficiently random sampling of the whole Earth throughout the Precambrian and Palaeozoic.

[6] Compared with Phanerozoic rocks, the palaeomagnetic database of Archaean rocks is very small. The Archaean shields of Canada, particularly the Superior Province, are the most extensively studied with 40 entries in the GPMDB, [*Zhai et al.*, 1994; *McElhinny and Lock*, 1996; *Buchan et al.*, 1998], followed by Africa, Europe, and Australia (16, 11, and 8 entries in the GPMDB, respectively). Only a few studies convincingly demonstrate the timing of magnetization through several field tests. For instance, *Meert et al.* [1994] show by means of a positive fold, reversal, and conglomerate tests that a succession of the Nyanzian System (Tanzania Craton), carries an NRM of 2680 ± 10 Ma. However, many studies lack palaeomagnetic field tests and/or precise age control. Previous palaeomagnetic studies of Archaean rocks were mostly focused on a single rock formation within a specific area and resulted in one palaeopole for that area [e.g., *Morimoto et al.*, 1997; *Wingate*, 1998]. When combined, results from these studies determine an apparent polar wander path (APWP) that is poorly constrained, with average time gaps of circa 60 Myr between following palaeopoles [*Idnurm and Giddings*, 1988]. Compared to many Phanerozoic APWPs (e.g., Laurentia, one key pole position per 20.8 Myr from the Early Cambrian to present, based on more than 3000 pole positions [cf. *van der Voo*, 1990; *McFadden and McElhinny*, 1995; *McElhinny and McFadden*, 2000]) these Archaean APWPs are extremely crude and would be deemed meaningless in a Phanerozoic context. Therefore to obtain meaningful Archaean APWPs, it is essential to study precisely dated Archaean successions within one geologically coherent terrain and preferably within a coherent stratigraphic section.

[7] Over the last 20 years the sensitive high-resolution ion microprobe (SHRIMP) has revolutionized Precambrian geochronology by providing ages commonly with precisions of only a few million years. When these ages are integrated into detailed geological and geophysical studies of Archaean terrains they provide a framework that is becoming suitable for high-precision palaeomagnetic studies, as we illustrate in this study.

[8] The circa 2775–2715 Ma Nullagine and Mount Jope Supersequences [*Blake*, 1993, 2001] in the Nullagine Synclinorium in the Pilbara Craton of Western Australia (Figures 1 and 2) were chosen for this study because they comprise a well-exposed, relatively undeformed and unaltered late Archaean succession that contains an abundance of flood basalts. In addition, the succession in the study area (Figures 1 and 2) has recently been divided (stratigraphically) in detail and has been precisely dated (Figure 3) [*Blake*, 2001; T. S. Blake et al., Stratigraphic geochronology of a late Archaean flood basalt province in the Pilbara Craton, Australia: Constraints on basin evolution, mafic and felsic volcanism and continental drift rates, submitted to *Precambrian Research*, 2003; hereinafter referred to as Blake et al., submitted manuscript, 2003].

[9] There are few previous palaeomagnetic studies of the Nullagine and Mount Jope Supersequences and associated igneous intrusions. *Embleton* [1978] presented the first palaeopole for the Black Range Dyke (Figure 1) and the Cajuput Dyke, (SCD in Figure 2) which are part of the Black Range Suite that has now been dated at 2772 ± 2 Ma by *Wingate* [1999], SHRIMP U-Pb zircon). *Embleton* [1978] interpreted the NRM as primary based on a positive baked contact test. *Schmidt and Embleton* [1985] presented palaeomagnetic data for the Mount Roe basalt (Figure 4) and the Mount Jope Volcanics (broad equivalents of the Kylena basalt to Maddina basalt in Figure 4), as well as for the older Millindinna Complex (Figure 1) that was dated at 2860 ± 20 Ma by *Gulson and Korsch* [1983]. *Schmidt and Embleton* [1985] interpreted the NRM preserved in the rocks as primary based on positive fold tests. *Schmidt and Clark* [1994] carried out a palaeomagnetic study of the banded-iron formations (BIFs) of the Hamersley Range Megasequence, which overlies the Chichester Range Megasequence. The rocks studied are dated between 2479 ± 3 Ma (SHRIMP U-Pb, zircon [*Nelson*, 1999]) and 2449 ± 3 Ma (SHRIMP U-Pb, zircon [*Barley et al.*, 1997]). They found remagnetized pole positions, which they interpreted to have been caused by burial metamorphism. The age of remagnetization of the BIFs was estimated by *Schmidt and Clark* [1994] at 2200 ± 100 Ma based on a positive fold test on folds formed during the Ophthalmia Orogeny. *Sumita et al.* [2001] presented the results of a study of BIF of the Hamersley Province (Beasley River region; Figure 1) and basalts of the Mount Jope Supersequence in the southern Pilbara. They found that both the BIF and their basalt samples are remagnetized and have not preserved any primary NRM directions.

[10] The most extensive relevant work in the Pilbara recently is by *Li et al.* [2000]. This work has focused mostly on the BIFs of the Hamersley Province, though some basalts of the Mount Jope Supersequence were also sampled. *Li et al.* [2000] distinguished five phases of remanent magnetization. The bulk of their samples revealed

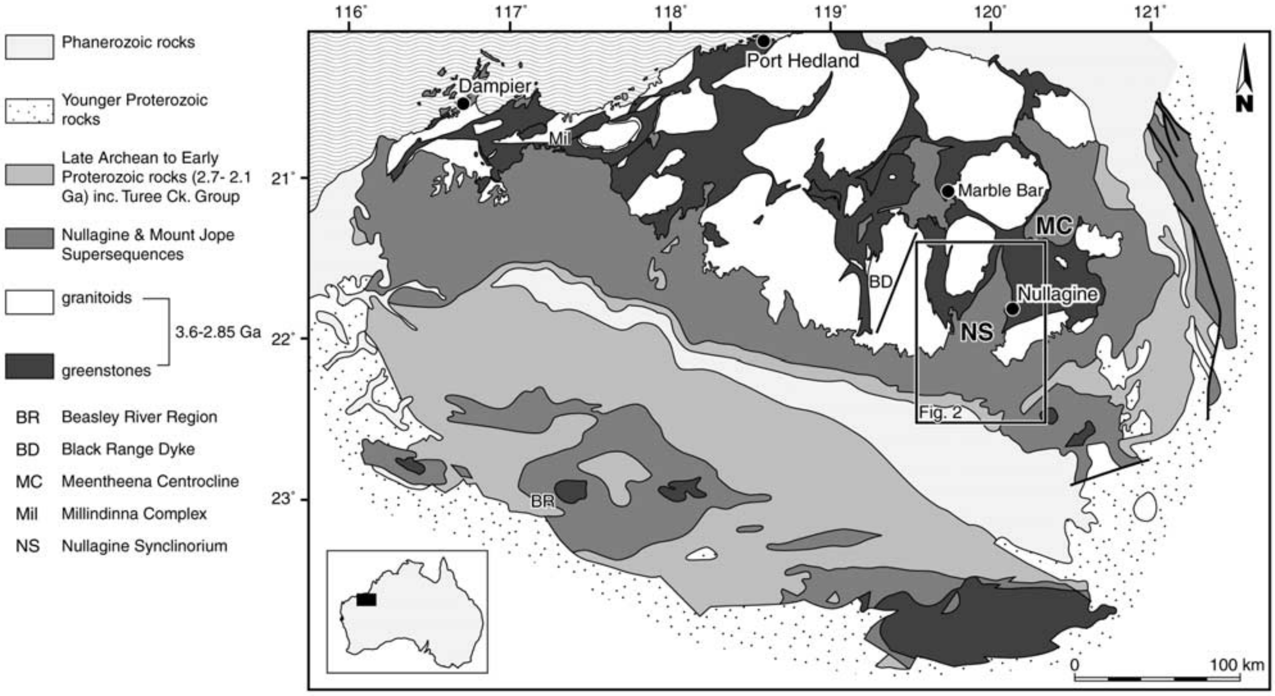

Figure 1. Simplified geological map of the Pilbara, showing the locations of the Beasley River Region, the Black Range Dyke, the Meentheena Centrocline, the Millindinna Complex, the Nullagine Synclinorium, and the approximate location of Figure 2. The Hamersley Province comprises most of the southwestern half of the map.

overprinted directions, possibly obtained during either the Ophthalmian (<2.45-circa 2.2 Ga) or the Ashburton (1.8–1.65 Ga) Orogenies. *Li et al.* [2000] note that separating Ophthalmian-related structures from Ashburton-related structures is difficult. Thus there is a large degree of uncertainty as to the ages of their magnetic overprint directions. *Li et al.* [2000], however, did record a possible primary NRM direction in basalt samples from the Chichester Range Megasequence, but this was not tested.

[11] To summarize, palaeomagnetic studies of the Hamersley Range Megasequence have revealed only remagnetized NRM directions, whereas the Chichester Range Megasequence and associated dolerite dykes appears to have preserved a primary NRM.

2. Aims of the Study

[12] Important aims of our palaeomagnetic study are summarized as follows: (1) to demonstrate that there is a primary NRM in the succession; (2) to test the proposed correlations by *Blake* [2001] between mafic dykes and flood basalts in the area; (3) to establish a magnetostratigraphy for a late Archaean flood basalt succession; (4) to look for evidence of geomagnetic reversals in the succession; and (5) to establish a series of palaeomagnetic poles within a single, coherent stratigraphic succession for the period 2775–2715 Ma and thus to construct a high-precision APWP for the Pilbara Craton for this time period.

3. Geological Setting

[13] The Mount Bruce Supergroup is a late Archaean to Early Proterozoic succession of volcanic and sedimentary rocks, unconformably overlying the circa 3.5–2.85 Ga "granite-greenstone" terrain of the Pilbara Craton. The Supergroup has been divided into three groups, which, from old to young, are the Fortescue Group, the Hamersley Group, and the Turee Creek Group [e.g., *MacLeod et al.*, 1963; *Trendall*, 1979; *Thorne and Trendall*, 2001]. An unconformity-based framework for part of the lower succession of the Hamersley Province (i.e., most of the Fortescue Group or the Nullagine and Mount Jope Supersequences; Figures 1 and 4) was initiated in the 1980s to early 1990s [see *Blake*, 1993]. More recently, *Blake* [2001] extended the unconformity-based divisions in the Nullagine Synclinorium of the east Pilbara and this framework is followed herein (Figures 2, 3, and 4; see *Blake* [1993, 2001] for details).

[14] The regional geotectonic evolution of the Nullagine and Mount Jope Supersequences is presented in detail by *Blake* [1993, 2001] and is summarized as follows. The two supersequences are interpreted as the rock record of a two-phase continental breakup in the late Archaean. The first phase, represented by the Nullagine Supersequence, was dominated by WNW-ESE directed extension (in present coordinates) that resulted in the formation of large volumes of mostly subaerial basalt, followed by the development of extensional intracontinental sedimentary basins with associated felsic and mafic volcanics, and an ocean may have formed to the west of the present craton. The second phase of breakup, represented by the Mount Jope Supersequence, involved rifting of the southern Pilbara Craton margin, possibly along an earlier transfer fault, resulting in the eruption of large volumes of basalt, with minor felsic volcanism. In the north, the craton was buried beneath subaerial flood basalts and mafic tuff piles, whereas in the

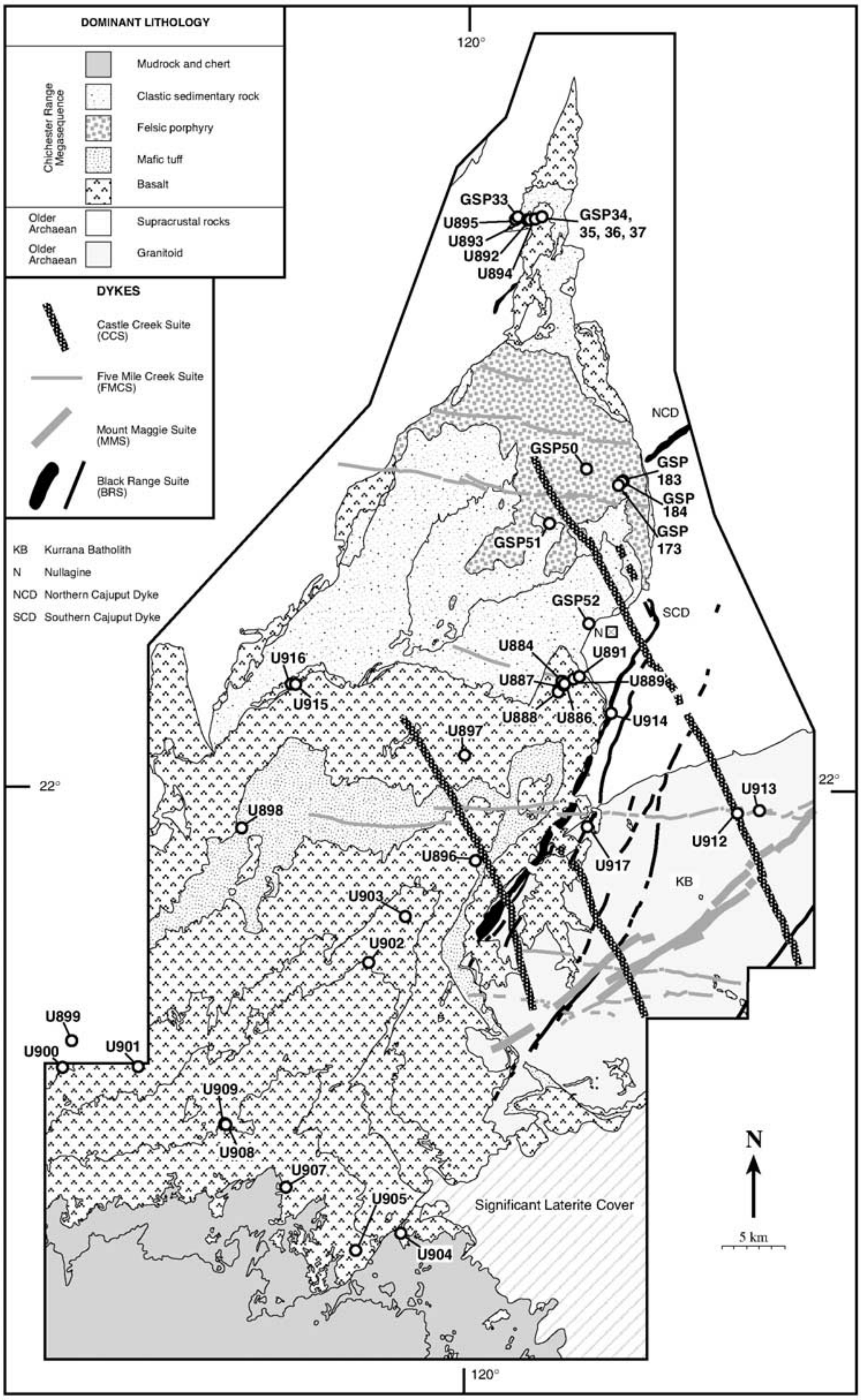

Figure 2. Summary geological map of the Nullagine Synclinorium showing dominant lithologies, related mafic dykes [after *Blake*, 2001], and sample locations (see Table 1).

south it was buried beneath a dominantly submarine mafic succession.

[15] Figures 2 and 3 summarize the geology of the Nullagine and Mount Jope Supersequences (and part of the Marra Mamba Supersequence Package) in the Nullagine Synclinorium. The succession comprises basalt, porphyritic felsic lava domes (?), mafic and felsic tuffs, and terrigenous clastic sedimentary rock. It is metamorphosed to very low grade (prehnite-pumpellyite-epidote zone (<200 mPa, <300°C) [*Smith et al.*, 1982]), gently folded by two gen-

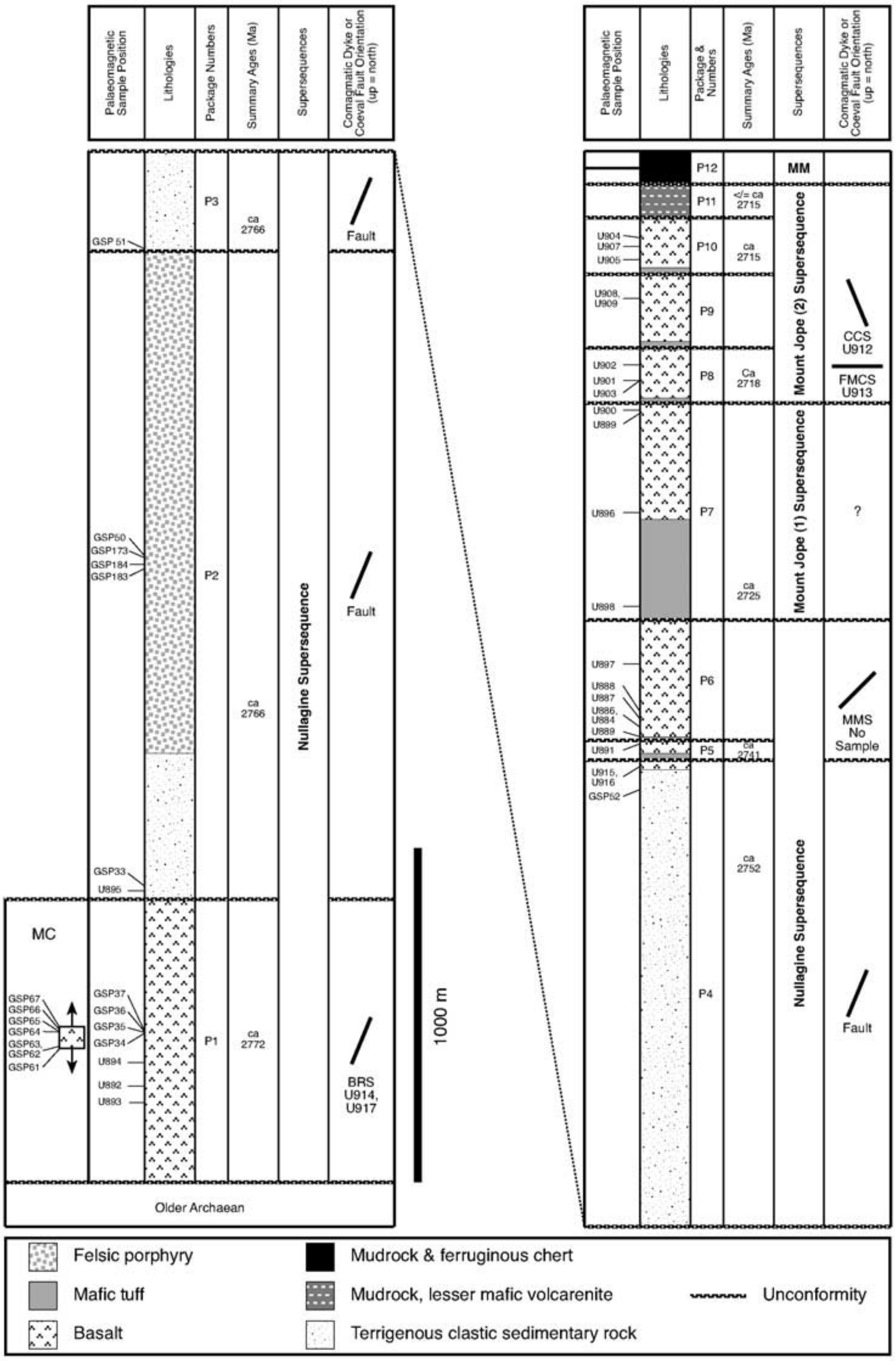

Figure 3. Summary stratigraphic column (cumulative maximum stratigraphic thickness) of the Nullagine and Mount Jope Supersequences and the lower Marra Mamba Supersequence package in the Nullagine Synclinorium [after *Blake*, 2001]. The figure includes (from left to right) the approximate stratigraphic position of the Meentheena Centrocline Package 1 samples (GSP61-67), the stratigraphic position of palaeomagnetic sample sites in the Nullagine Synclinorium, dominant lithologies, package numbers, summary rock ages, second-order divisions, and comagmatic dyke and growth-fault orientations (with palaeomagnetic sample site numbers). Correlations with the lithostratigraphic scheme and a regional stratigraphic context are given in Figure 4. Each basalt sample number tie line represents a single flow unit; two basalt sample sites with a single tie line represent two sample sites in the same flow unit. The exact stratigraphic positions of Sites GSP 34–37 were not recorded but they are shown in their correct relative stratigraphic positions. Positions of samples GSP50, GSP 173, GSP183, and GSP 184 are estimates of their positions within the stratigraphic section of the dacite porphyry. BRS, Black Range Suite; CCS, Castle Creek Suite; FMCS, Five Mile Creek Suite; MC, Meentheena Centrocline; MM, Marra Mamba Supersequence Package; MMS, Mount Maggie Suite.

UNCONFORMITY-BASED DIVISIONS				LITHOSTRATIGRAPHIC DIVISIONS	
Chichester Range Megasequence, Regional Subdivisions (Blake, 1993)	**Chichester Range Megasequence Subdivisions in the East Pilbara Basin (Blake, 1993)**	**Chichester Range Megasequence in the Nullagine Synclinorium (East Pilbara Basin) (Blake, 2001)**		**Mount Bruce Supergroup in the Nullagine Synclinorium**	**Mount Bruce Supergroup in the Nullagine Synclinorium**
2nd Order Subdivisions or Grouped 2nd Order Subdivisions	**3rd Order Subdivisions or Grouped 3rd Order Subdivisions**	**Super-sequences**	**Package Number**	**Formations and Members**	**Groups**
Marra Mamba Supersequence Package			Package 12	Marra Mamba Iron Formation	Hamersley Group
				Jeerinah Formation and basal Woodiana Member	Fortescue Group
			Package 11		
Mount Jope Supersequence	Maddina Sequence Package	Mount Jope (2) Ss	Package 10	Maddina Basalt	
				Kuruna Member	
			Package 9	Maddina Basalt	
			Package 8		
	Tumbiana Sequence	Mount Jope (1) Ss	Package 7	Tumbiana Formation	
	Kylena Sequence	Nullagine Supersequence	Package 6	Kylena Basalt	
			Package 5		
Nullagine Supersequence	Taylor Creek Sequence (Hardey Seq. Package)		Package 4	Hardey Sandstone	
			Package 3		
	Hales Grave Well Sequence (Hardey Seq. Package)		Package 2	Hardey Sandstone & “quartz-plagioclase porphyry”	
	Mount Roe Sequence		Package 1	Mount Roe Basalt	
PILBARA CRATON (OLDER ARCHAEAN)					

Figure 4. A comparison of stratigraphic subdivisions of the lower succession of the Hamersley Province in the Nullagine Synclinorium [after *Blake*, 2001]. The right two columns are after *Hickman and Lipple* [1978], *Thom et al.* [1979], and *Thorne and Tyler* [1996]. Sequence stratigraphic/lithostratigraphic correlations are simplified.

Table 1. Summary of High Temperature Results From the Nullagine Synclinorium and the Meentheena Centrocline[a]

Area	Package/Dyke	Site Number	Lithology	AMG Coordinates (AGD 84)	*N*	*n*	Dec	Inc	*K*	α95	R	Plat	VGP Lat	VGP Long
NS	10	U904	basalt	50K 0803892-7529581	10	10	152.6	46.7	52.3	6.7	9.828	27.9	−64.6	191.5
NS	10	U907	basalt	50K 0794956-7533268	10	8	147.2	48.6	49.4	8.0	7.858	29.6	−59.7	189.0
NS	10	U905	basalt	50K 0800384-7528231	12	8	158.9	55.9	77.0	6.4	7.909	36.4	−66.9	167.5
NS	**10 mean**				**3**	**26**	**153.3**	**52.1**	**243.5**	**7.9**	**2.992**	**31.3**	**−64.1**	**183.5**
NS	9	U908	basalt	50K 0790365-7538167	14	0	n/a	n/a	n/a	n/a	n/a	n/a	n/a	n/a
NS	9	U909	basalt	50K 0790358-7538230	15	4	149.0	39.3	19.7	21.2	3.848	22.3	−61.4	203.9
NS	**9 mean**				**1**	**4**	**149.0**	**39.3**	**n/a**	**n/a**	**n/a**	**22.3**	**−61.4**	**203.9**
KB	CCS	U912	dolerite	51K 0211344-7562821	27	14	127.0	53.5	102.9	3.9	13.874	34.0	−42.2	183.6
KB	**CCS mean**				**1**	**14**	**127.0**	**53.5**	**n/a**	**n/a**	**n/a**	**34.0**	**−42.2**	**183.6**
NS	8	U902	basalt	50K 0801760-7550680	11	2	147.2	43.4	n/a	n/a	1.997	25.3	−59.9	197.3
NS	8	U901	basalt	50K 0783579-7542746	10	7	141.5	50.0	342.6	3.3	6.982	30.8	−54.7	187.4
NS	8	U903	basalt	50K 0804763-7554167	15	10	142.2	50.5	80.6	5.4	9.888	31.2	−55.2	186.6
NS	**8 mean**				**3**	**19**	**143.2**	**48.0**	**292.1**	**7.2**	**2.993**	**29.1**	**−56.7**	**190.1**
KB	FMCS	U913	mafic-rich dolerite	51K 0213166-7563166	36	19	155.8	58.0	40.2	4.8	18.526	38.7	−63.4	165.9
KB	**FMCS mean**				**1**	**19**	**155.8**	**58.0**	**n/a**	**n/a**	**n/a**	**38.7**	**−63.4**	**165.9**
NS	7	U900	basalt	50K 0777731-7542868	10	10	175.9	77.2	884.4	1.6	9.990	65.6	−46.6	122.2
NS	7	U899	basalt	50K 0778502-7544894	11	8	132.0	75.7	564.4	2.3	7.988	63.0	−38.2	145.1
NS	7	U896	basalt	51K 0190962-7558533	10	3	164.4	57.9	47.8	18.0	2.958	38.6	−68.8	155.5
NS	7	U898	mafic tuff	50K 0792063-7561302	10	7	181.3	72.6	62.6	7.7	6.904	57.9	−54.1	118.7
NS	**7 mean**				**4**	**28**	**160.8**	**71.7**	**56.3**	**12.3**	**3.947**	**56.3**	**−52.8**	**133.7**
NS	6	U897	basalt	50K 0809522-7566847	10	5	104.6	67.0	49.6	11.0	4.919	49.7	−25.9	164.1
NS	6	U888	basalt	51K 0197002-7571844	10	0	n/a	n/a	n/a	n/a	n/a	n/a	n/a	n/a
NS	6	U887	basalt	51K 0197465-7572443	10	0	n/a	n/a	n/a	n/a	n/a	n/a	n/a	n/a
NS	6	U886	basalt	51K 0197449-7572544	10	4	165.9	61.7	96.8	9.4	3.969	42.9	−66.0	146.1
NS	6	U884	basalt	51K 0197264-7572677	10	0	n/a	n/a	n/a	n/a	n/a	n/a	n/a	n/a
NS	6	U889	basalt	51K 0198233-7572870	11	0	n/a	n/a	n/a	n/a	n/a	n/a	n/a	n/a
NS	5	U891	basalt	51K 0198573-7573091	10	2	170.7	77.4	n/a	n/a	n/a	65.9	−45.6	125.5
NS	**5 & 6 mean**				**3**	**11**	**145.6**	**71.4**	**28.9**	**23.4**	**2.931**	**52.8**	**−47.1**	**147.1**
NS	4	U915	basalt	50K 0796304-7572341	26	7	167.6	75.1	120.4	5.5	6.950	62.0	−49.1	128.7
NS	4	U916	basalt	50K 0796058-7572405	5	0	n/a	n/a	n/a	n/a	n/a	n/a	n/a	n/a
NS	4	GSP52	mafic tuff	51K 0199348-7577225	9	0	n/a	n/a	n/a	n/a	n/a	n/a	n/a	n/a
NS	**4 mean**				**1**	**7**	**167.6**	**75.1**	**n/a**	**n/a**	**n/a**	**62.0**	**−49.1**	**128.7**
NS	3	GSP51	terrigenous mudrock	51K 0196019-7584831	4	0	n/a	n/a	n/a	n/a	n/a	n/a	n/a	n/a
NS	**3 mean**				**0**	**0**								
NS	2	GSP50	massive dacite porphyry	51K 0198794-7589321	14	10	332.4	−70.1	29.2	9.1	9.692	54.1	51.5	326.0
NS	2	GSP173	massive dacite porphyry	51K 0201271-7588274	7	7	318.4	−74.7	78.4	6.9	6.923	61.3	41.2	325.2
NS	2	GSP184	Massive dacite porphyry	51K 0201617-7588455	7	1	313.6	−63.7	n/a	n/a	n/a	45.3	45.6	346.8
NS	2	GSP183	Massive dacite porphyry	51K 0201729-7588543	7	0	n/a	n/a	n/a	n/a	n/a	n/a	n/a	n/a
NS	**2 mean**				**3**	**18**	**320.9**	**−69.7**	**153.7**	**10.0**	**2.987**	**53.6**	**46.5**	**332.7**
NS	2	GSP33	conglomerate containing Package 1 basalt clasts	51K 0192952-7608690	40	26	n/a	n/a	n/a	n/a	n/a	n/a	n/a	n/a
NS	2	U895	conglomerate containing Package 1 basalt clasts	51K 0192871-7608499	10	0	n/a	n/a	n/a	n/a	n/a	n/a	n/a	n/a
MC	1	GSP67	basalt	51K 0212666-7628329*	7	6	130.1	73.0	255.9	4.2	5.980	58.6	−38.6	151.0
MC	1	GSP66	basalt	51K 0212666-7628329*	7	7	142.1	71.5	4898.0	0.9	6.999	56.2	−45.4	149.4
MC	1	GSP65	basalt	51K 0212666-7628329*	7	6	136.6	67.2	748.0	2.5	5.993	49.9	−45.6	159.5
MC	1	GSP64	basalt	51K 0212666-7628329*	7	5	137.9	70.7	117.2	7.1	4.966	55.0	−44.1	152.6
MC	1	GSP63	basalt	51K 0212600-7628194*	7	7	129.1	70.5	161.5	4.8	6.963	54.7	−39.6	155.8
MC	1	GSP62	basalt	51K 0212600-7628194*	7	6	132.9	70.4	175.6	5.1	5.972	54.5	−41.7	154.9
MC	1	GSP61	basalt	51K 0212600-7628194*	7	7	129.4	66.5	1014.7	1.9	6.994	49.0	−41.6	162.9
NS	1	GSP37	basalt	51K 0194857-7608645*	5	4	124.8	60.2	481.8	4.2	3.994	41.1	−39.9	173.8
NS	1	GSP36	basalt	51K 0194857-7608645*	5	0	n/a	n/a	n/a	n/a	n/a	n/a	n/a	n/a
NS	1	GSP35	basalt	51K 0194857-7608645*	5	0	n/a	n/a	n/a	n/a	n/a	n/a	n/a	n/a

Table 1. (continued)

Area	Package/Dyke	Site Number	Lithology	AMG Coordinates (AGD 84)	N	n	Dec	Inc	K	α95	R	Plat	VGP Lat	VGP Long
NS	1	GSP34	basalt	51K 0194857-7608645*	5	2	126.3	71.4	n/a	n/a	1.973	56.1	−37.8	154.8
NS	1	U894	basalt	51K 0194425-7608523	10	7	125.7	63.3	139.1	5.1	6.957	44.8	−40.1	168.9
NS	1	U892	basalt	51K 0194045-7608483	10	7	120.2	58.3	327.0	3.3	6.982	39.0	−36.5	176.8
NS	1	U893	basalt	51K 0193839-7608409	10	10	129.1	70.0	176.0	3.7	9.949	53.9	−40.0	156.6
NS + MC	**1 mean**				**12**	**74**	**129.6**	**67.9**	**231.0**	**2.9**	**11.952**	**51.1**	**−41.2**	**159.9**
NS	BRS	U914	gabbro	51K 0201215-7570357	5	0	n/a	n/a	n/a	n/a	n/a	n/a	n/a	n/a
NS	BRS	U917	dolerite	51K 0199583-7561500	19	3	120.9	69.7	190.8	8.9	2.990	53.5	−35.8	159.1
NS	**BRS mean**				**1**	**3**	**120.9**	**69.7**	**n/a**	**n/a**	**n/a**	**53.5**	**−35.8**	**159.1**

[a]Results are in stratigraphic order, with each comagmatic dyke placed at the base of its associated package. Meentheena Package 1 data are placed above the Nullagine data (in stratigraphic order) for convenience only; exact correlations are uncertain. Correlation of Meentheena Package 1 and Nullagine Package 1 basalts is based on relative stratigraphic position, flow morphologies, and petrographic characteristics. Bold type indicates means. Abbreviations: AMG, Australian Map Grid; *N*, number of specimens from each site and number of sites contributing to the mean; *n*, number of specimens accepted and the number of specimens contributing to the mean; dec, declination; inc, inclination; Plat, palaeolatitude; VGP lat (long), latitude (longitude) of VGP; n/a, not applicable; KB, Kurrana Batholith; MC, Meentheena Centrocline; NS, Nullagine Synclinorium; CCS, Castle Creek Dyke Suite; FMCS, Five Mile Creek Suite; BRS, Black Range Suite. Identical AMGs with asterisk indicate sequences of sites in basalt flows directly on top of each other. Dec, Inc, α95, Plat, VGP Lat and VGP Long in degrees.

erations of folds, and cut by a complex array of normal faults [*Blake*, 2001].

[16] The approximate 6-km-thick (cumulative maximum thickness) succession has been divided into 11 unconformity-bound packages and an upper package with a basal unconformity (Figure 3). The packages have been numbered sequentially from oldest to youngest. Each package is interpreted as a cogenetic unit, but, importantly, packages are not hierarchically identical. Package 1 is dominated by subaerial basalt, Package 2 is dominated by clastic sedimentary rock and felsic porphyry, and Packages 3 and 4 are dominated by clastic sedimentary rock with minor subaerial basalt near the top of Package 4 [*Blake*, 1993, 2001]. Packages 5–10 are dominated by basalt and mafic tuff but also contain minor felsic tuff bands. Package 11 is a marine succession that comprises mostly laminated mudrock with subordinate reworked crystal-rich felsic tuff, carbonated mafic volcarenite, and chert. Package 12 is a marine succession that comprises laminated carbonaceous mudrock that passes gradationally upward into ferruginous laminated chert.

[17] In addition to extrusive mafic rocks, there are four physically and geochemically distinct mafic dyke suites in the area, each with a characteristic orientation (Figure 2). These are the Black Range Suite [*Blake*, 1993] and the Mount Maggie, Five Mile Creek, and Castle Creek Suites [*Blake*, 2001]. Each dyke suite has been matched geochemically to basalts within the Nullagine or Mount Jope Supersequences in the Nullagine Synclinorium by *Blake* [2001].

[18] Initial dating of the Hamersley Province succession was dominated by the use of the Rb-Sr whole rock and mineral isochron methods, which yielded mostly mean ages of 2300–2000 Ma [see summaries by *Trendall*, 1983; *Blake and McNaughton*, 1984; see also *Nelson et al.*, 1992]. *Pidgeon* [1984] published the first conventional zircon U-Pb age of 2768 ± 16 Ma for the felsic porphyry in Package 2 in the Nullagine Synclinorium (Figure 3), and *Arndt et al.* [1991] provided the first SHRIMP zircon U-Pb ages for the Fortescue Group. These zircon U-Pb ages established a broad geochronological framework and showed that Rb-Sr and Pb-Pb isochrons obtained from igneous rocks probably date younger hydrothermal and/or metamorphic events rather than the age of magmatism [*Blake and McNaughton*, 1984; *Nelson et al.*, 1992].

[19] *Wingate* [1999] determined a mean ion microprobe baddeleyite $^{207}Pb/^{206}Pb$ age of 2772 ± 2 Ma from four samples, each from a different dyke of the Black Range Suite including the Black Range Dyke itself. Geochemical and geological correlations [*Blake*, 2001] suggest that Package 1 basalt in the Nullagine Synclinorium is comagmatic with the Black Range Suite and hence is of the same age (Figure 3). Blake et al. (submitted manuscript, 2003) [see *Blake*, 2001] have obtained 11 high-precision SHRIMP zircon U-Pb ages from rocks within the Nullagine Synclinorium covering Packages 2–11. Package 2 is dated at circa 2766 Ma [cf. *Pidgeon*, 1984], the upper part of Package 4 is dated at circa 2752 Ma, Package 5 is dated at circa 2741 Ma, and Packages 7–10 were deposited between circa 2725 and 2715 Ma (Figure 3).

4. Sampling

[20] Four hundred and seventy-one oriented drill cores (25 mm diameter, 5–6 cm long) were taken from the

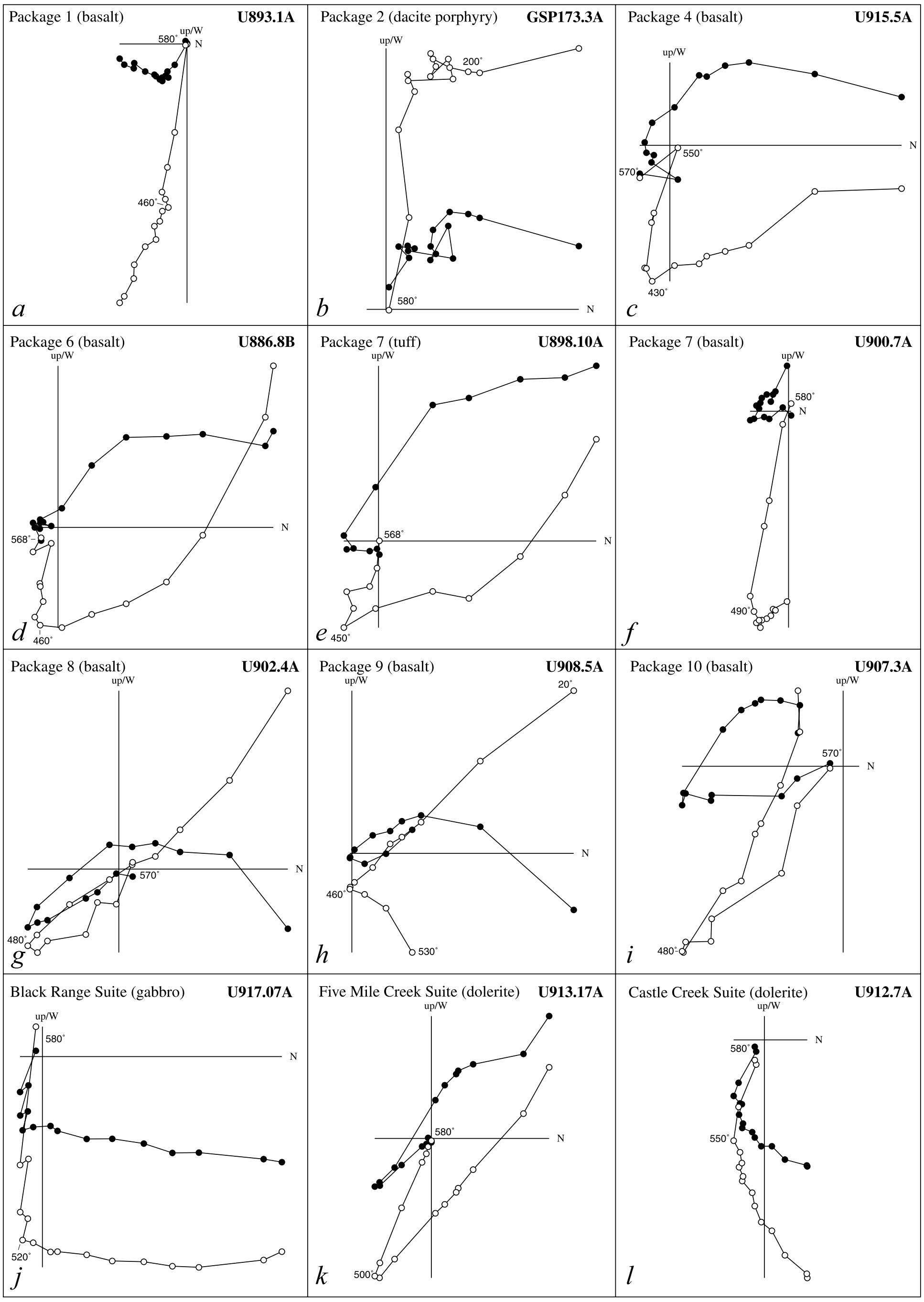

Figure 5. Examples of characteristic Zijderveld diagrams from each package and sampled comagmatic dykes. Key temperature steps are shown. Specimen numbers indicate location (Figure 2 and Table 1) followed by sample number. Figures 5a, 5b, 5f, 5h, 5j, 5k, and 5l show two components of magnetization, and Figures 5c, 5d, 5e, 5g, and 5i show three components.

supracrustal succession in the Nullagine Synclinorium and associated comagmatic dykes in the area (Figure 3 and Table 1). Mafic dyke samples were taken from the Black Range, Five Mile Creek, and Castle Creek Suites (Figure 3) [*Blake*, 2001]. The Mount Maggie Suite (Figure 3) [*Blake*, 2001] was not sampled because it is poorly exposed. Samples were collected using a petrol drill, with an average of nine cores per site for the supracrustal succession. Four oriented hand samples were collected (Site GSP51) and cored in the laboratory (two cores per hand sample). In addition, to enable a fold test for Package 1, 49 cores were collected from 7 sites from basalts of a stratigraphic equivalent to Package 1 in the Meentheena Centrocline (Figures 1, 3, and 4).

[21] Sample sites were chosen carefully to allow collection of fresh in situ rock in areas least likely to have been struck by lightning. Most supracrustal samples are of flood basalts, with fewer samples from massive dacite porphyry, terrigenous mudrock, mafic tuff, and conglomerate (Table 1). Packages 5 and 6 were sampled as one unit because the

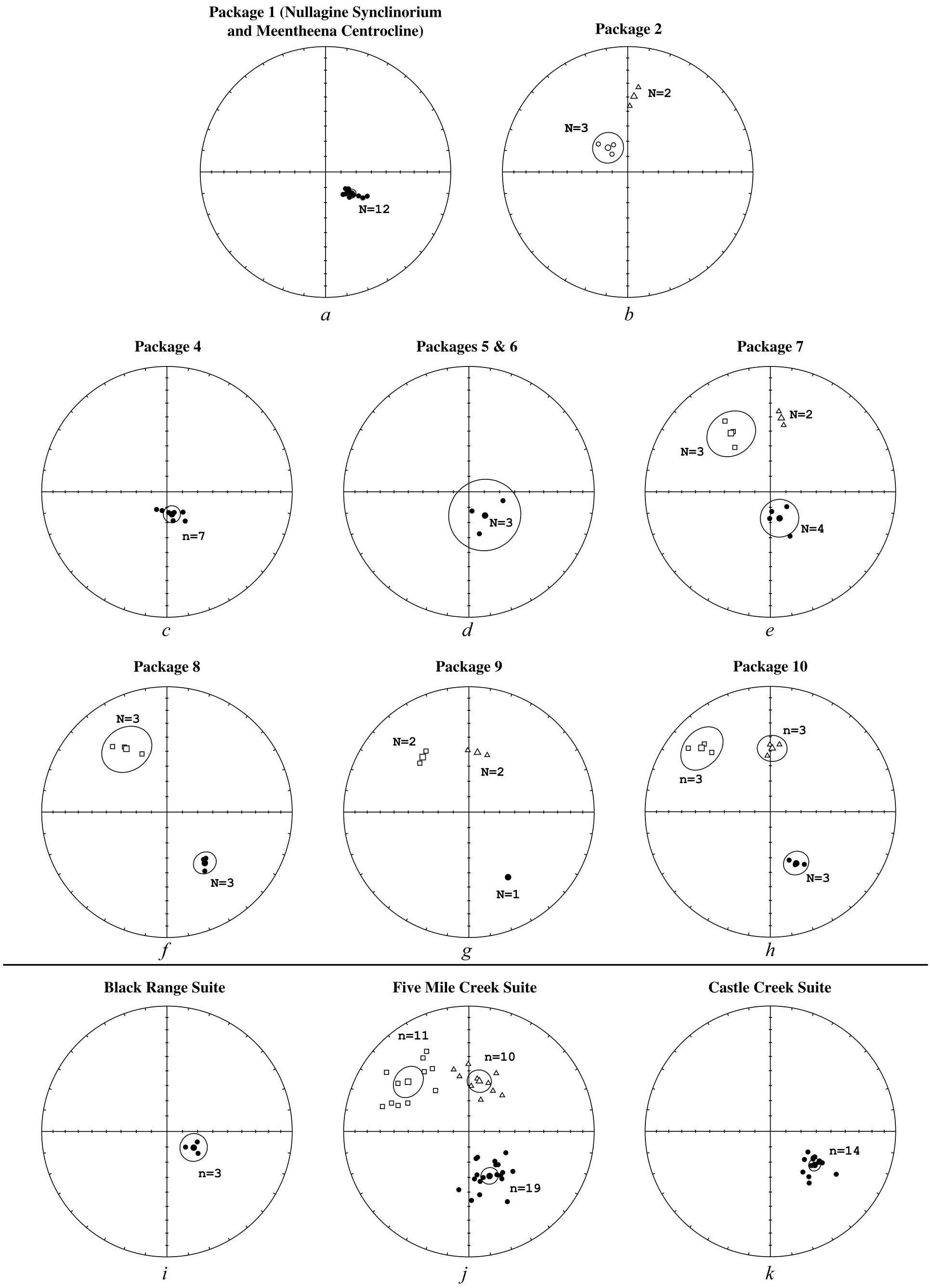

Figure 6. Equal-area plots of results from all studied packages and dykes. Figures 6a, 6b, 6d, 6e, 6f, 6g, and 6h represent equal-area plots of multiple sites. *N*, total number of sites with accepted data, small symbols are site means, larger symbols are the mean of site means with the corresponding $\alpha95$ circles (where applicable). Figures 6c, 6i, 6j, and 6k represent single sites, *n*, total number of specimens, larger symbols are the sample means showing error circles. Open (solid) symbols indicate negative (positive) inclinations, circles are high-temperature directions, squares are medium-temperature directions, and triangles are low-temperature directions. Data are shown in Tables 1 and 2.

distinction between these packages had not been made at the time of sampling.

5. Methods

[22] In the field, a susceptibility meter (Scintrex K2) was used as an indication for magnetic intensity of the sampled rocks in the field. For low values, a magnetic compass was used to orient the samples, and for higher values, as a precaution a sun compass was used in addition to the magnetic compass. No significant difference was recorded between magnetic and sun compass directions (between 0° and 2° in all cases).

[23] In the laboratory, the cores were cut to standard specimens of 22-mm length. The anisotropy of magnetic susceptibility was measured on an AGICO KLY 3 suscep-

tibility bridge, which showed that the samples are not significantly anisotropic (range from 0.3 to 3.4%). At least one specimen and occasionally two specimens of each drill core were thermally demagnetized in a magnetically shielded, laboratory-built furnace. The NRM was measured on a 2G Enterprises DC superconducting quantum interference device (DC-SQUID) cryogenic magnetometer. Eleven specimens were demagnetized using the alternating field (AF) technique, where demagnetization was performed in a laboratory-built AF demagnetizer up to a peak field of 200 mT.

[24] NRM directions were analyzed and interpreted with Zijderveld diagrams [*Zijderveld*, 1967]. Principal component analysis [*Kirschvink*, 1980] was used to determine the directions of the various NRM components. Mostly, no directions with a maximum angular deviation (MAD) greater than 10° were used, except for very weak samples.

6. Results

6.1. Thermal Demagnetization

[25] The NRM of all rock units shows either two or three components. A low-temperature (LT) component was recorded in the temperature range of 20° to 300°–350°C; this component was well developed in Packages 2, 7, 9, and 10 and in the Five Mile Creek Suite. A medium-temperature (MT) component was recorded from 350°C to approximately 450°C; this component is well developed in specimens from Package 7 upward and in the Five Mile Creek Suite. A high-temperature (HT) component was recorded from 450° to 580°C; this component is well developed in almost all rock units and rock types, except in Packages 3 and 9.

[26] The LT component records the present-day field direction (Figures 5 and 6), which is generally only apparent in samples with a weak magnetic intensity of the HT component. All samples are of fresh rock, so the LT present-day field component is unlikely to be caused by weathering. Possibly, a (small) part of the NRM has been reset in the ambient field by high surface rock temperatures (air temperatures commonly exceed 40°C in summer) and is recorded by low coercivity or low unblocking temperature magnetite. For example, the normalized intensity versus temperature plot of sample U892.2A (Figure 7c) shows a two-step intensity decay, with 20% intensity loss between the 20° and 300°C steps, which is when the LT component unblocks. Between 300° and 500°C only a gradual intensity decrease is observed and from 500°C the HT component effectively starts unblocking in this sample.

[27] The following paragraphs describe the palaeomagnetic results per package and dyke suite. Confer Table 1 for statistical details.

[28] Package 1 has a well-developed HT component and magnetizations of relatively high magnetic intensity (on average 50 × 10^{-3} A m^{-1}, whereas most packages have an average magnetic intensity of 5–10 × 10^{-3} A m^{-1}, although compared to modern basalts, these intensities are all exceptionally low). Except for Sites GSP35 and GSP36, which have been affected by lightning, the distribution of high-temperature directions from both the Nullagine Synclinorium and Meentheena Centrocline samples is very well clustered (Figure 6a). LT and MT components were poorly developed or did not have consistent directions in this package (e.g., Figure 5a).

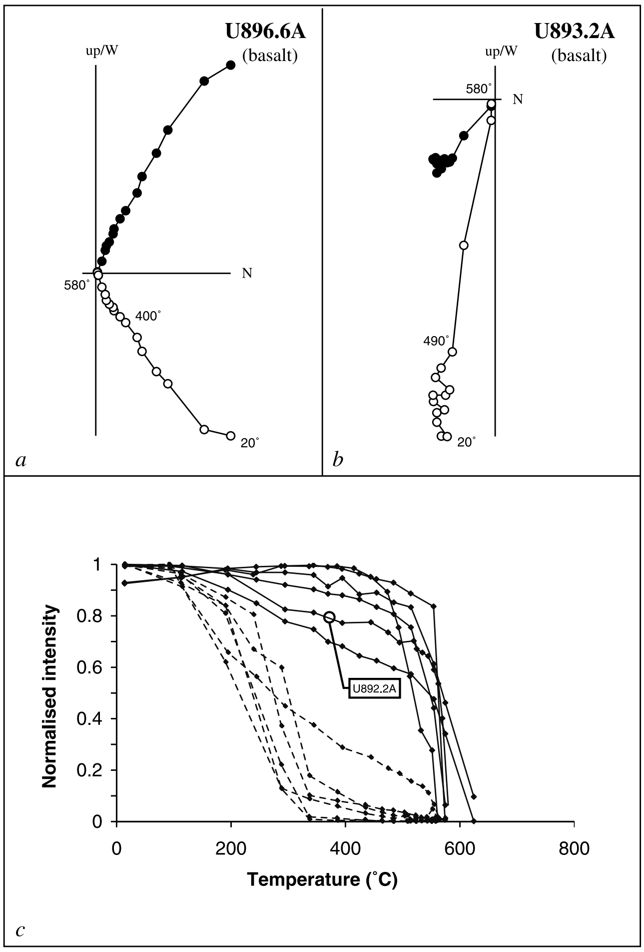

Figure 7. Examples illustrating the effects of lightning strikes. (a) Zijderveld diagram of a basalt sample struck by lightning, showing a characteristic steep intensity decrease at low temperatures. (b) Zijderveld diagram of a basalt sample not struck by lightning, showing a gradual intensity decrease up to 490°C followed by a steep decrease up to 580°C. (c) Normalized intensity versus temperature of selected basalt samples. The dashed lines show the intensity decay of representative samples struck by lightning (specimens U894.10, U896.6, U915.11, .15, .16, and .19). Solid lines show the intensity decay of samples not struck by lightning (specimens U892.2, .7A, and .7B, U893.1, .2, and .5, and U899.5). Specimen U892.2 is pointed out to show two-step unblocking: the LT component unblocks between 20° and 300°C and the HT component unblocks between 500° and 580°C. Conventions of Figures 7a and 7b as in Figure 5, see Figure 2 for specimen locations.

[29] The Package 2 felsic porphyry showed an HT component with a consistent direction, which is antipodal to the HT components of other packages (Figures 5b and 6b). The MT directions were poorly defined, and the LT directions could rarely be determined.

[30] Most exposed rocks in Package 3 were unsuitable for palaeomagnetic sampling. An attempt was made to acquire data from a siltstone (GSP51) but no reliable HT components were derived.

[31] In Package 4, a mafic tuff horizon (GSP52), and a single basalt flow (U915, U916) near the top of this succession were sampled. The mafic tuff revealed only present-day field directions and was unsuitable for thermal demagnetization (i.e., they exploded above 350°–400°C). Four specimens of the basalt flow revealed a low-temperature present-day field direction (e.g., Figure 5c) and only seven specimens revealed a consistent HT direction (Figure 6c). The remaining samples from this package were affected by lightning.

[32] No well-defined component could be derived from basalt samples from Packages 5 to 6 because the HT component is largely overprinted by an MT component of inconsistent direction, resulting in an unreliable end vector at high temperatures. Out of seven sites, with a total of 71 samples (Table 1), only three sites, with a total of 11 samples, revealed meaningful results (e.g., Figure 6d).

[33] Most samples of Package 7 were taken from flood basalts and one sample set was taken from a mafic tuff (U898). Individual sites show a good clustering of the data (e.g., Site U899, with k = 564, Table 1), but the package mean direction has a larger spreading (k = 56, Table 1). In the flood basalts, except for Site U896, all three NRM components are developed (Figures 5e and 5f) and cluster well (Figure 6e). While some mafic tuff samples are affected by a present-day field overprint, the MT and HT components are clearly present.

[34] In Package 8, the MT and HT directions form well-defined clusters, and the present-day field overprint is generally poorly developed, but some samples show all three NRM components, as illustrated in Figure 5g. Data from individual sites cluster well as does the package mean, both for the HT and MT directions.

[35] Suitable fresh exposure of Package 9 basalt was not found in the Nullagine Synclinorium. The basalt is commonly strongly weathered because of its coarse grain size [*Blake*, 2001, Table 6]. Despite this problem, the few samples from a single basalt flow unit in Package 9 (Figure 3) yielded all three NRM components (e.g., Figures 5h and 6g). The MT component is well developed at both sites, although the HT component is only consistent at Site U909 (Figure 6g).

[36] In Package 10, all three components of magnetization are recorded (e.g., Figure 5i) and their directions form well-defined clusters (Figure 6h). Occasionally, the NRM could not be completely removed, giving scattered directions at temperatures of 560°C or higher, possibly because of growth of new magnetic minerals during thermal demagnetization.

[37] The Black Range Suite was sampled at two locations (U914, U917). The Cajuput Dyke (Figure 2; Site U914) was difficult to drill because it contains abundant quartz. The few samples from this site revealed only a present-day field direction. A smaller dyke from the same suite (Site U917) is finer grained. The demagnetization diagrams for this site generally show an HT and an LT component (e.g., Figure 5j), of which only a few consistent and reliable HT directions could be derived (Figure 6i). The LT directions do not cluster.

[38] The Five Mile Creek Suite was sampled at one location (Site U913), and all three magnetization components are present (e.g., Figure 5k). The HT component is commonly present and its directions cluster reasonably (k = 40), while also the LT and MT components form acceptable clusters (Figure 6j).

[39] The Castle Creek Suite was sampled at one location (Site U912) and shows MT and HT components of magnetization (Figure 5l). The MT component is poorly developed and does not cluster, whereas the HT component is easily distinguished and its directions show clear clustering (Figure 6).

6.2. Lightning

[40] Previous work has shown that exposed rocks in the Pilbara have commonly been struck by lightning [*Schmidt and Embleton*, 1985; *Schmidt and Clark*, 1994]. Lightning strikes can destroy or partly reset NRM [*Hallimond and Herroun*, 1933]. Lightning strikes have been shown to disturb the remanent magnetization of a surface area by as much as 25 m^2 [*Graham*, 1961] and can affect rocks down to 25 m below the surface. However, the original remanent magnetization can usually be detected at a depth of 90–160 cm in areas struck by lightning. Since lightning commonly strikes on high and/or open places, sampling sites were chosen in narrow and deep-cutting gullies or on steep rock faces.

[41] Following several pilot studies (T. van Hoof, personal communication, 1997), careful field procedures have resulted in only 10% of the samples showing a lightning-induced remanent magnetization. Lightning has the following effects on NRM, which proved to be diagnostic in the recognition of lightning-induced NRM.

[42] 1. The intensity of the magnetic signal is usually much stronger (commonly by more than an order of magnitude) than the intensity of the magnetic signal of the same rock unaffected by lightning.

[43] 2. Samples affected by lightning generally reveal only one component (e.g., compare Figure 7a with Figure 7b).

[44] 3. The direction of this one component compared to other samples from the same site or location is random, so sampling an area around a point which has been struck by lightning should reveal a set of random directions [*Graham*, 1961].

[45] 4. The (normalized) magnetic intensity is observed to decrease rapidly with increasing temperature, whereas the magnetic intensity of (magnetite bearing) rocks unaffected by lightning shows a gradual decrease until about 525°–550°C and then a steep decrease close to 580°C (Figure 7c).

6.3. Field Tests

[46] To help constrain the time at which the NRM was acquired, three palaeomagnetic field tests were carried out, namely a fold test, a reversal test, and a conglomerate test.

[47] A fold test could not be achieved in the Nullagine Synclinorium because the succession dips too shallowly (mostly <5°) and is only gently folded. However, HT data from Package 1 in the Nullagine Synclinorium can be compared with HT data from a stratigraphic equivalent of Package 1 in the Meentheena Centrocline (Figure 1) to define a fold test. Directions before and after tilt correction are shown in Figure 8a (data in Table 1). These data do not pass the fold test according to definition 1 of *McFadden* [1990] because statistically the two groups do not belong to

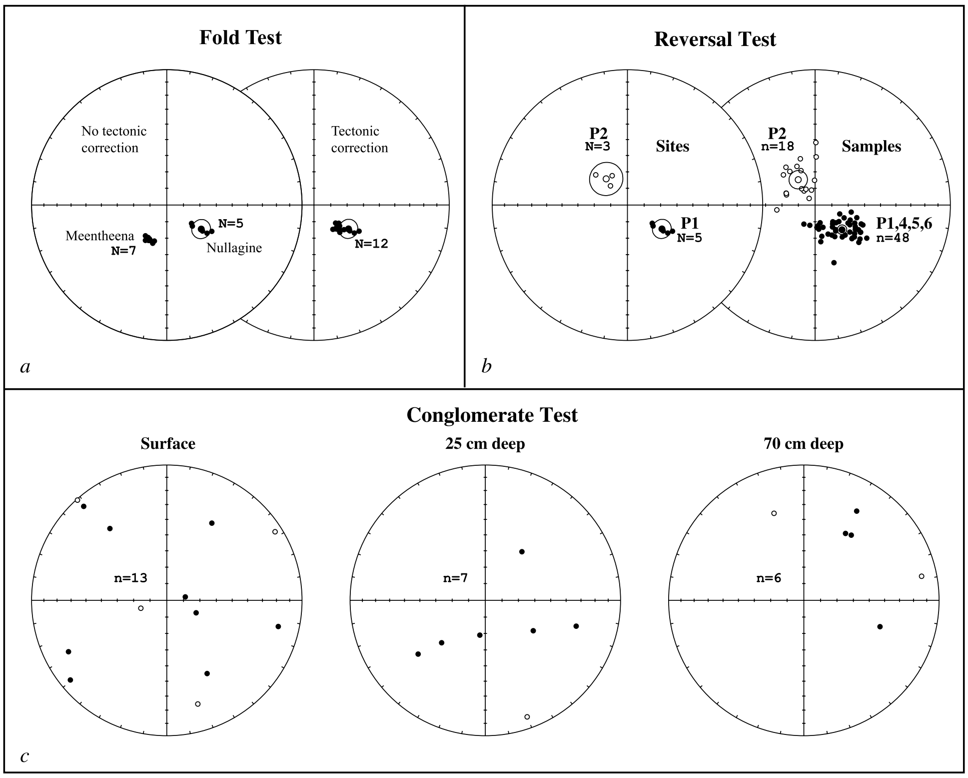

Figure 8. (a) Equal-area plots of HT directions from the fold test before and after tilt correction. Symbols represent site means. All directions are from Package 1, both from the Nullagine Synclinorium and from the Meentheena Centrocline. The α95 circle of the Meentheena data are too small (1.9°) to be noticed on the plot. (b) Equal-area plots of HT directions from the reversal test. The left plot shows the directions of site averages of Packages 1 and 2 in the Nullagine Synclinorium; the right plot shows the directions of individual samples of Packages 1, 2, 4, and 5–6 from the Nullagine Synclinorium. (c) Equal-area plots of HT directions from the conglomerate test, taken at three different levels. All directions are from specimens of Package 2, Site GSP33 (Figure 2). Conventions as in Figure 6.

the same population, but in an incremental fold test using an eigenvector approach, they do give better results at 100% tilt correction [*Tauxe and Watson*, 1994]; but the best result is obtained at approximately 130 ± 30% unfolding. The large error is caused by the small difference in bedding between Nullagine and Meentheena. One problem in applying the McFadden fold test is that the precision parameter of the Meentheena samples (k_1 = 806) is much higher than that of the Nullagine samples (k_2 = 182; so k_1/k_2 = 4.4). Ideally, the k_1/k_2 ratio should not be larger than 2. A second problem is determination of the exact dip of shallow dipping basalt flows. Flow tops are commonly undulose at several scales, and tectonic dips are difficult to estimate accurately. This may explain the misfit of site means after tilt correction in Figure 8a. However, because the incremental tilt correction gives better results at 100% unfolding, we conclude that the HT magnetization was most probably acquired prior to folding. The age of the folding is not exactly known. *Blake* [2001] describes that NNE trending folds are thought to have formed contemporaneously with the development of the Nullagine and Mount Jope Supersequences. The age of the SE trending folds is more problematic, but a Mount Jope Supersequence age cannot be excluded.

[48] The discovery of magnetic reversals in the HT component of the succession allowed for a reversal test, which was carried out using two different approaches. First, the HT site means of Package 1 (Nullagine Synclinorium and Meentheena Centrocline data) were compared to those of Package 2 and the reversal test of *McFadden and McElhinny* [1990] was performed (Figure 8b, left). With and without simulation the reversal test was found to be positive (classification B), meaning that the antipodal angle lies between 5° and 10°. The angle between the mean of the normal and the mean of the reversed polarity set is 8.0°, which is smaller than the critical angle of 9.2°. Second, a reversal test was performed on all accepted individual HT sample directions from Packages 1 to 6 (except for the Package 2 conglomerate samples; Figure 8b, right). This reversal test is also positive, with the angle between the mean of the normal and the mean of the reverse polarity set being 6.0°, which is lower than the critical angle of 6.2°(resulting in classification B). Although no data are available for the sedimentary successions of Packages 3 and 4, the reversed interval is stratabound, which is additionally suggestive of a primary magnetization.

[49] A conglomerate test was carried out on basalt clasts (cobbles to boulders) in a conglomerate that overlies Package 1 basalts. Field relationships, petrographic data, and unpublished geochemical data show that the basalt clasts were derived from Package 1 basalts. Basalt clasts were sampled (one core per clast) and thermally demagnetized (Table 1). The succession above the conglomerate was also

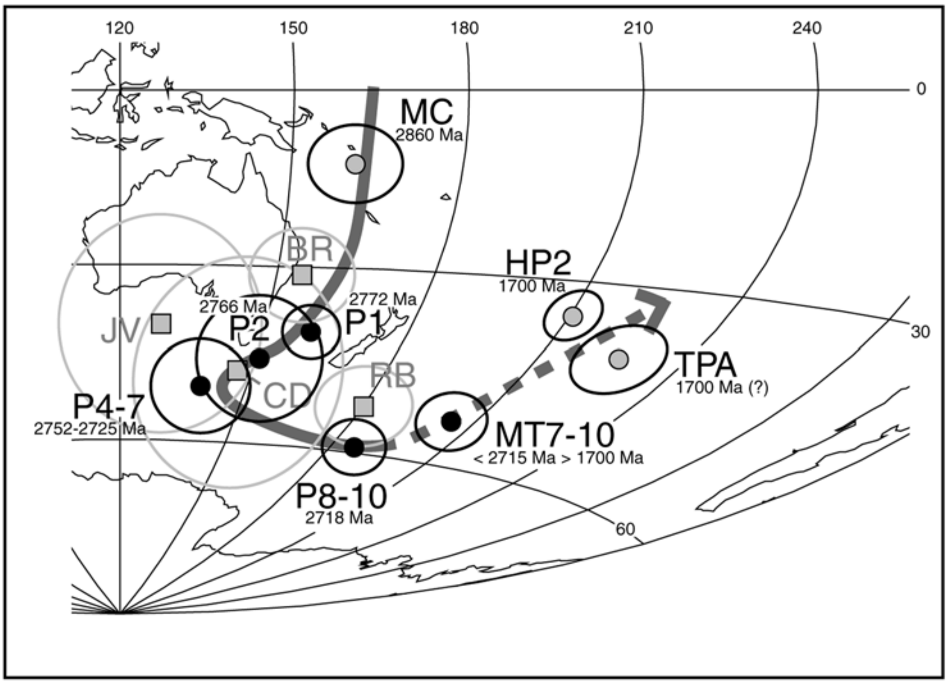

Figure 9. Aitoff projection of the apparent polar wander path (APWP) for the Pilbara from circa 2860 to circa 1700 (?) Ma showing approximate pole ages. Dashed part of the APWP is speculative. The APWP is based on this study and published data. Square symbols are poles not included in the APWP. Circular symbols are poles included in the APWP, of which the black solid circles are poles from this study. Poles comprising the APWP are MC (Millindinna Complex [*Schmidt and Embleton*, 1985]), P1 (Nullagine and Meentheena Package 1 HT data and the Black Range Suite HT data), P2 (Package 2 HT data), P4–7 (Packages 4–7 HT data), P8–10 (Packages 8–10 HT data and Five Mile Creek Suite and Castle Creek Suite HT data), MT7-10 (medium-temperature directions), TPA (Mt. Tom Price iron ore [*Schmidt and Clark*, 1994]), and HP2 (Hamersley Province F3 pole [*Li et al.*, 2000]). Each package pole is a grouped mean of the mean site data, including comagmatic dykes (cf. Table 3). Poles not included in the path are BR (Black Range Dyke) and CD (Cajuput Dyke [*Embleton*, 1978]), RB (Mount Roe basalt) and JV (Mount Jope Volcanics, [*Schmidt and Embleton*, 1985]).

sampled (Package 2 massive dacite porphyry to Package 10), making this conglomerate test an intraformational conglomerate test [*McElhinny and McFadden*, 2000]. The test was carried out at two sites approximately 100 m apart. The characteristic remanent magnetization (ChRM) of specimens from the first site (U895; Figures 2 and 3) shows no preferred orientation. However, from the strong magnetic intensity of these samples and from the intensity decay curves we interpret these samples as having been struck by lightning.

[50] The second site (GPS33; Figures 2 and 3) was sampled at the surface and, following blasting, at depths of 25 and 70 cm below the original surface (Figure 8c). Samples from basalt clasts at this site mostly have much lower magnetic intensities than the U895 basalt clast samples. In addition, the magnetic intensity of these basalt clasts was mostly two orders of magnitude lower than the intensities of the underlying Package 1 basalts, an observation similar to that of *Shipunov et al.* [1998]. Of a total of 40 samples, 14 (35%) are interpreted as affected by lightning. Of the 21 basalt clasts sampled at the surface, 8 (38%) are affected by lightning. At 25 cm below the surface, 3 (30%) of the 10 clast samples are affected by lightning. At 70 cm below the surface, three (33%) of the nine clast samples are affected by lightning. Hence blasting to a depth of 70 cm made little difference to the percentage of samples affected by lightning.

[51] The ChRM of the samples of GSP33 from the surface that were not affected by lightning has no preferred orientation (Figure 8c). The test for uniform randomness of *Watson* [1956] requires the resultant (R) of all N individual directions to be smaller than a critical value R_0. In this case, $N = 13$, $R_0 = 5.75$, and $R = 3.150$, so $R < R_0$, meaning that there is at least a 95% probability that the directions come from a random population. Further, an alternative and more sensitive conglomerate test by *Shipunov et al.* [1998], which allows for the inclusion of a known secondary component or reference vector for the studied area, is also positive, with $\rho_0 = 0.263$ and $\rho = 0.207$, so $\rho < \rho_0$. The reference vector used in the calculations is 132.5°/68.0°, the average direction of NRM of Packages 1, 4, and 5–6.

[52] The ChRMs from 25 cm below the surface give a negative Watson test for uniform randomness and the test of Shipunov was also negative, with $N = 7$, $R_0 = 4.18$, $R = 4.939$, $\rho_0 = 0.362$, and $\rho = 0.686$ (Figure 8c). The ChRMs from the 70 cm below the surface also did not pass the Watson test for uniform randomness, with $N = 6$, $R_0 = 3.85$, and $R = 4.211$. However, the test of Shipunov with $\rho_0 =$

Table 2. Summary of Medium Temperature Results From the Nullagine Synclinorium[a]

Package/Dyke	Site Number	*N*	*n*	Dec	Inc	*k*	α95	R	Plat	VGP Lat	VGP Long
10	U904	10	6	315.7	−25.5	24.9	13.7	5.800	13.4	47.1	34.1
10	U907	10	8	315.3	−34.0	34.2	9.6	7.795	18.6	48.1	26.4
10	U905	12	3	307.7	−18.4	19.0	29.1	2.895	9.4	38.3	35.6
10 mean		**3**	**17**	**312.7**	**−26.0**	**84.2**	**13.5**	**2.976**		**not calculated**	
9	U908	5	3	324.8	−40.3	56.6	16.5	2.965	23.0	57.6	21.7
9	U909	5	3	314.9	−43.9	345.8	6.6	2.994	25.7	48.8	15.8
9 mean		**2**	**6**	**320.0**	**−42.2**	**n/a**	**n/a**	**1.995**		**not calculated**	
8	U902	11	6	326.9	−38.0	103.0	6.6	5.951	21.3	59.3	25.1
8	U901	10	3	333.5	−46.0	63.6	15.6	2.969	27.4	65.4	12.2
8	U903	15	8	320.3	−31.6	97.1	5.6	7.928	17.1	52.4	30.3
8 Mean		**3**	**17**	**327.3**	**−39.8**	**64.6**	**15.5**	**2.969**		**not calculated**	
FMS	U913	36	11	310.1	−35.1	24.6	7.6	10.556	19.4	43.4	23.9
FMS Mean		**1**	**11**	**310.1**	**−35.1**	**n/a**	**n/a**	**n/a**		**not calculated**	
7	U900	10	7	327.3	−33.4	25.8	12.1	6.767	18.2	59.1	31.0
7	U899	11	7	321.3	−52.6	23.2	12.8	6.742	33.2	54.2	3.3
7	U896	10	0	n/a	n/a	n/a	n/a	n/a	n/a	n/a	n/a
7	U898	10	6	328.3	−43.0	21.4	14.8	5.766	25.0	60.8	17.7
7 Mean		**3**	**20**	**326.0**	**−43.0**	**66.5**	**15.2**	**2.970**		**not calculated**	
Total MT		**12**	**71**	**320.0**	**−37.1**	**52.0**	**6.1**	**11.788**	**20.7**	**53.2**	**23.9**

[a]Consistent MT directions were found only in Packages 7, 8, 9, and 10 and the FMCS. Results are grouped by package and comagmatic dyke suite. See Table 1 for additional sample data and explanation of abbreviations. Dec, Inc, α95, Plat, VGP Lat and VGP Long in degrees.

0.392 and ρ = 0.258 is positive. When all accepted samples from the surface, 25- and 70-cm depth are pooled, both the test of Watson ($N = 26$, $R_0 = 8.18$, and $R = 9.621$) and the test of Shipunov ($\rho_0 = 0.186$ and $\rho = 0.348$) are negative.

[53] The results of the conglomerate test after the blasting are unclear, and it is possible that the ChRM has been (partly) reset by the shock wave from the blasting (shock-induced remagnetization?). Although the clasts from 70 cm below the surface pass the test of Shipunov, the negative results from 25 cm below the surface make the validity of the data after the blasting uncertain and are thus disregarded. However, since the ChRM in the basalt clasts not struck by lightning from the surface is random, the conglomerate test is interpreted as positive. Together with the positive fold test and positive reversal test, we conclude that the ChRM preserved in the rocks from Packages 1 to 10 is a primary NRM.

[54] Thus the HT component of the accepted basalt, dolerite, and dacite porphyry samples is interpreted to have been acquired during or shortly after the cooling of the rocks in the late Archaean and is a record of the geomagnetic field at that time. The HT component of the accepted mafic tuff samples (U898) is interpreted as the result of lock-in of free magnetite grains during consolidation of the tuff and is also a record of the geomagnetic field in the late Archaean.

7. Discussion

7.1. Dyke to Package Correlations

[55] From earlier palaeomagnetic correlations it could be deduced that the Black Range Suite (BR in Figure 9) was possibly of similar age as the Chichester Range Megasequence. This follows from data presented by *Schmidt and Embleton* [1985], although they used a different lithostratigraphic terminology. New geochemical evidence shows that the Black Range Suite is most probably comagmatic with Package 1 [*Blake*, 2001]. This is supported by the palaeomagnetic data presented herein (Table 1). Further, the Five Mile Creek Suite correlates geochemically to Package 8 and the Castle Creek Suite to Package 9 or 10 [*Blake*, 2001]. From our palaeomagnetic data, these correlations are less apparent (Table 1), but when the results of Packages 8–10 are averaged as one group (see below), the Five Mile Creek and Castle Creek Suite results fall in this group and do not contradict the proposed correlations. More sampling of the dykes is needed, however, to convincingly confirm the proposed correlations palaeomagnetically.

7.2. MT and HT Components

[56] The evaluation of all package means, including both the HT and the MT directions (if applicable), with their corresponding α95 made it apparent that there are five distinct groups of data (Tables 1 and 2) which have significantly different mean directions (Table 3). These groups are (1) P1, which comprises the HT directions of Package 1 samples plus the HT directions of Black Range Dyke Suite samples; (2) P2, which comprises the HT directions of Package 2 samples; (3) P4-7, which comprises the HT directions of Packages 4–7 samples; (4) P8-10, which comprises the HT directions of Packages 8–10 samples plus the HT directions of the Five Mile Creek Suite and the Castle Creek Suite samples; and (5) MT7-10, which comprises the MT directions of Packages 7–10 plus the MT directions of the Five Mile Creek Suite samples (Table 2).

[57] On the basis of the positive field tests, the HT component is interpreted as the primary NRM. It follows therefore that the age of the HT component is the same as the age of cooling of the basalt, dolerite, and dacite porphyry samples. These ages have been determined by high-precision geochronology and bracket the ages of the four HT groups as follows. P1 magnetization is circa 2772 Ma, P2 is circa 2766 Ma, P4-7 is bracketed between circa 2752 Ma and circa 2725 Ma, and P8-10 is bracketed between circa 2718 Ma and circa 2715 Ma (Figure 9).

[58] The direction of the MT component is in all cases reversed with respect to the direction of the HT component and has a relatively shallow inclination, in contrast to the relatively steep inclination of the HT components. Whereas

Table 3. Summary of Grouped Palaeolatitude and Palaeopole Positions From This Study and From Previously Published Data[a]

Group	*N*	Dec	Inc	Min Lat	Max Lat	Av Lat	Latp	Longp	α95	*dp*	*dm*
TPA	1	308.8	−9.3	0.0	10.6	4.7	−37.4	220.3	n/a	5.7	11.3
HP2	9	304.2	−18.1	6.9	11.8	9.3	−35.3	211.9	3	n/a	n/a
MT7-10	12	320.0	−37.1	16.7	25.2	20.7	−53.2	203.9	5.3	n/a	n/a
JV	5	n/a	n/a	n/a	n/a	n/a	−40.5	128.7	n/a	19.9	20.8
P8-10	9	146.8	49.9	26.2	35.7	30.7	−59.1	186.3	6.1	n/a	n/a
P4-7	8	157.5	72.2	46.2	70.6	57.3	−50.4	138.2	12.5	n/a	n/a
P2	3	320.9	−69.7	40.6	70.0	53.5	−46.5	152.7	15.2	n/a	n/a
P1	13	129.0	68.0	47.4	55.0	51.1	−40.8	159.8	3.7	n/a	n/a
CD	9	145.0	71.0	38.7	78.1	55.4	−46.0	146.0	22.0	n/a	n/a
BR	16	115.0	72.0	48.3	67.0	57.0	−32.0	154.0	9.0	n/a	n/a
RB	*4* (*12*)	320.0	−53.8	28.5	41.2	34.3	−52.4	178.0	n/a	6.4	9.1
MC	*1* (*8*)	265.0	−65.1	40.8	54.4	47.1	−11.9	161.3	n/a	6.8	8.4

[a]Group name in bold type indicates positions summarized in this study; group name in nonbold type indicates positions summarized in previously published data. Group definitions are given in the caption to Figure 9 and in the text. Site means contributing to each group mean are given in Tables 1 and 2, and each group is plotted in Figure 9. *N* is the number of sites contributing to the grouped mean (site means given in Tables 1 and 2). Site number in italic type is the number of localities, with number of sites in parentheses. Abbreviations: dec, declination; inc, inclination; min lat, minimum palaeolatitude; max lat, maximum palaeolatitude; av lat, average palaeolatitude; latp, latitude of pole position; longp, longitude of pole position; α95, confidence circle at the 95% level; *dp* and *dm* define the oval of 95% confidence about the mean pole. All units in degrees.

the HT directions of Packages 7 and 8 are clearly different (Table 1), the MT directions are similar, and therefore all MT directions are grouped in MT7-10. Hence MT7-10 is interpreted as the result of a (re)magnetization that is younger than the HT magnetization. Remagnetization in the Pilbara has previously been ascribed to either burial metamorphism [e.g., *Schmidt and Clark*, 1994; *Sumita et al.*, 2001] and/or orogenic activity [e.g., *Li et al.*, 2000]. However, if the MT remagnetization was caused by the thermal effects of regional-scale burial metamorphism or a regional-scale orogenesis, it should have been detected throughout the succession, not in the upper four packages only. Because no data were acquired higher than Package 10, the full stratigraphic distribution of the MT component is unknown. While the MT component is interpreted as the result of a ‘‘thermal’’ event, the exact nature and scale of the event is unknown.

[59] *Li et al.* [2000] describe phases of remanence acquired possibly at the end of the Ophthalmian Orogeny (circa 2200 Ma) and during the late Ashburton Orogeny (circa 1700 Ma). The MT component of this study is different from both of these remagnetizations and hence cannot readily be ascribed to either orogenic phase with any certainty. The pole of the MT direction plots approximately midway between the P8-10 pole (circa 2715–2718 Ma) and the circa 1700 Ma pole of the Hamersley BIFs (TPA and HP2, Figure 9) [*Schmidt and Clark*, 1994; *Li et al.*, 2000]. However, appropriate field tests should be done before the age of the MT7-10 magnetization can be constrained more accurately and more confidently.

7.3. Apparent Polar Wander

[60] Table 1 is an overview of the HT component data of all sampled rock units. Table 2 summarizes the directions of MT7-10. Virtual geomagnetic pole (VGP) positions have been calculated for the HT and MT components, both from the mean of each site and from the mean of each package and dyke suite. The palaeomagnetic poles for the grouped data (Table 3), which were calculated from the VGPs of the site means, are plotted in Figure 9, which also includes previously published relevant palaeomagnetic poles (cf. also Table 3). Although P2 plots within the 95% confidence limit of both P1 and P4-7, its average pole position plots halfway between these groups.

[61] There is some overlap of the relevant part of the previous APWP and the new APWP of this study within their 95% confidence limit (Figure 9). The previous poles plot on the APWP, but in an inconsistent order. For instance, BR, CD, and RB in Figure 9 are all similar in age (analogues to P1, 2772 ± 2 Ma) yet plot on three distinctly different positions on the new APWP. BR and CD have overlap with the P1 pole, but RB overlaps with P8-10.

[62] In contrast, the palaeopoles from this study follow a consistent time path and have smaller errors (Table 3). These differences may be attributed to the limited number

Figure 10. (opposite) Mean palaeolatitudes for the Nullagine and Mount Jope Supersequences in the Nullagine Synclinorium and Package 1 of the Meentheena Centrocline. The lower right column shows site mean HT palaeolatitudes (in degrees) linked to the stratigraphic column. Sample site numbers in grey boxes indicate dykes, and site numbers in bold indicate Meentheena data. The upper right column shows site mean medium-temperature (MT) palaeolatitudes, with the site numbers in italics. HT and MT site means are in stratigraphic order, with dyke sites at the base of their comagmatic package. The exact position of the Meentheena data in this column is uncertain and has been placed above the Nullagine Package 1 data for convenience only. Site mean palaeolatitudes are represented by a circle with a horizontal bar representing the α95 [after *Fisher*, 1953]. Closed (open) symbols represent normal (reversed) intervals. Five groups of palaeolatitudes (four HT means, one MT mean) have been distinguished, and their means are the means of their constituent sites (see Table 3). Groups are defined in the text and in the caption to Figure 9. Group means are given by thick black vertical lines, and their α95 is given by the grey boxes. The five groups have been linked to the stratigraphic column by dashed lines. N indicates normal polarity, R indicates reversed polarity.

of localities, sites, or samples per site in previous studies, which resulted in larger errors on the mean average magnetic directions, and hence in less precise pole determinations. From the new APWP (Figure 9), it becomes apparent that there has been considerable rotation, from at least Package 1 to Package 7. The distance between P4-7 and P8-10 on the APWP resembles a phase of latitudinal drift.

7.4. Magnetostratigraphy

[63] Magnetostratigraphic schemes have been developed for many Phanerozoic flood basalt provinces and have

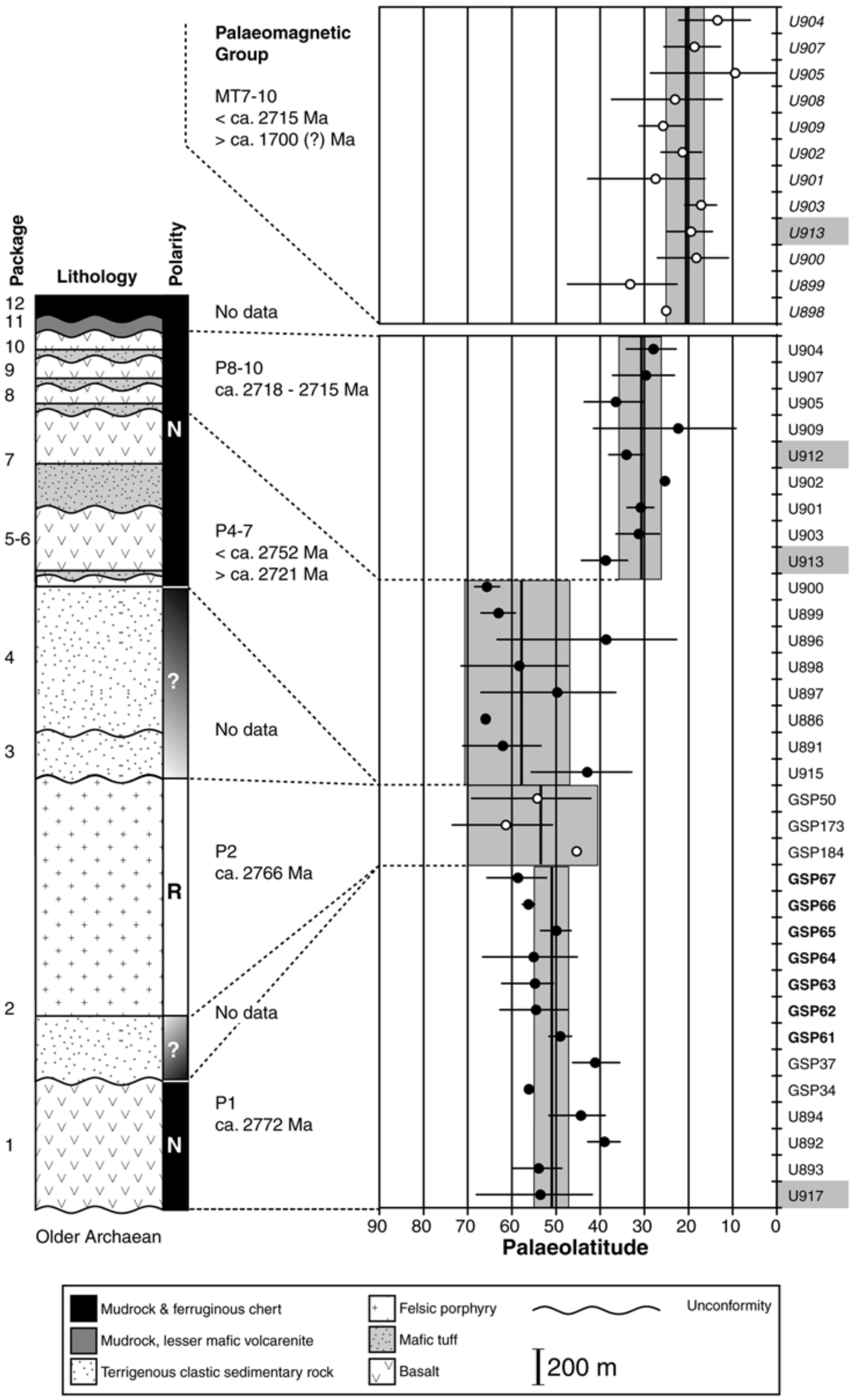

proven useful in stratigraphic divisions and correlations [e.g., *Reidel and Hooper*, 1989; *Marsh et al.*, 1997; *Saunders et al.*, 1997; *Westphal et al.*, 1998]. This paper presents the first magnetostratigraphic scheme for an Archaean flood basalt succession (Figure 10). Two particular components of this scheme may prove useful in assisting stratigraphic correlations within the Nullagine and Mount Jope Supersequences across the Pilbara Craton. These are (1) the normal-reverse-normal primary NRM up-stratigraphy (Figure 10) and (2) the major shift in palaeolatitude across the Package 7/8 boundary (Figure 10, see below).

7.5. Implications of Changes in Palaeolatitude

[64] The palaeolatitudes of individual site means and grouped means are plotted from oldest to youngest in Figure 10. Although the mean pole positions of groups P1, P2, and P4-7 differ, they have average palaeolatitudes that have overlapping errors, which implies that either no (significant) latitudinal movement has taken place or that it cannot be resolved with the current amount of data.

[65] There is a significant change in palaeolatitude (average 27.2°) at the Package 7/8 boundary between P4-7 and P8-10 (Figure 10). Geochemical data from the Nullagine Synclinorium show that this boundary also coincides with a major change in the composition of mafic rocks. For this reason, *Blake* [2001] split the Mount Jope Supersequence into two second-order packages in the Nullagine Synclinorium (Figure 4). The difference in mean SHRIMP zircon ages from above and below this boundary is 3 Myr (95% confidence error range of 0–10 Myr, (Blake et al., submitted manuscript, 2003). Assuming an Earth of current radius, the average shift is 3025 km, which in 3 million years gives a rate of shift of palaeolatitude of 100 cm per year. However, taking into account errors in average palaeolatitude and age, the maximum rate of shift is instantaneous motion (if Packages 7 and 8 are of the same age) and the minimum possible rate is a shift of 12 cm per year. Importantly, these are all minimum estimates since longitudinal shift is unconstrained.

[66] The geological meaning of this 27.2° shift in palaeolatitude is unknown, and fundamentally different explanations are possible depending on different assumptions. These are summarized as follows.

7.5.1. Option 1

[67] The Earth did not have a purely GAD in the late Archaean. Long-term contributions of nondipole fields and the change of this contribution through time could generate an apparent shift in palaeolatitude. For example, if an octupole contribution to the dipole field changed from 0 to 40%, this would result in an apparent latitudinal shift of $\sim$25° (cf. Figure 4 of *van der Voo and Torsvik* [2001]). The likelihood of long-term nondipole fields through geological time is a topic of debate [cf. *van der Voo and Torsvik*, 2001, and references herein], but as an option it cannot be ruled out. However, since the shift in palaeolatitude is sustained in Packages 9 and 10, a sudden change in octupole contribution (or other nondipole contribution) must have remained stable for at least circa 3 Myr. This interpretation has no precedent throughout geological history and is not regarded as the most likely option.

7.5.2. Option 2

[68] The shift in palaeolatitude is the result of true polar wander (TPW). The nature and validity of TPW is still a topic of debate. *Kirschvink et al.* [1997] argue that fast apparent motion of continents in the Cambrian was the result of a 6° Myr^{-1} shift of the Earth's spin axis with respect to the geographic reference frame. However, *Meert* [1999] finds no compelling palaeomagnetic support for this model, although the author states that a relatively small contribution of TPW cannot entirely be ruled out. *Courtillot and Besse* [1987] note that TPW is a continuous process and argue that TPW only comes to a standstill during periods of low reversal frequency and during episodes of continental breakup. Aspects of our data are not consistent with TPW being an explanation of the 27° shift in palaeolatitude. These include an apparent low reversal frequency (see below) and the relatively fast and sudden shift across the Package 7/8 boundary. While TPW cannot be discounted, observations to date do not support it as an explanation for the documented shift in palaeolatitude. As a special case, inertial interchange (II) TPW could explain the sudden shift in palaeolatitude. In this scenario, unbalance of the Earth's landmasses cause the lithosphere and mantle to rotate $\sim$90° with respect to the Earth's spin axis [cf. e.g., *Kirschvink et al., 1997*], which results in rapid TPW. (II)TPW is a topic of considerable controversy, which so far has not even been proven. Therefore we retain a conservative interpretation and we feel that the burden of proof is with the advocates of nondipole fields and/or (II)TPW.

7.5.3. Option 3

[69] The Earth had a GAD, and the latitudinal shift is the result of plate movement. Possible drift rates across the Package 7/8 boundary (as discussed above) range from fast Phanerozoic drift rates [e.g., *Meert et al.*, 1993] to drift rates that are up to an order of magnitude faster than any known Phanerozoic drift rate. In a Phanerozoic plate tectonic setting, rapid drift rates are commonly associated with fast spreading following continental rifting. *Blake and Barley* [1992] and *Blake* [1993] proposed a broad two-stage rifting to rifted setting for the development of the Nullagine and Mount Jope Supersequences. Their proposed first stage, represented by the Nullagine Supersequence, could not be confirmed by our palaeomagnetic data in terms of latitudinal drift because the palaeolatitude results of Packages 1–4 are not significantly different. However, there is evidence for rotation during this phase (Figure 9), as is confirmed by a change in declination from 129.0° in P1 to 157.5° in P4-7 (Table 3). However, their second stage of rifting is supported by our palaeomagnetic data. Indeed, the shift in palaeolatitude between Packages 7 and 8 was used by *Blake* [2001] to divide the Mount Jope Supersequence in the Nullagine Synclinorium into two parts (Figure 3). The recorded 3025 km of drift in a single event represents a phase of rapid horizontal movement.

[70] The cause(s) of this possible event is/are unknown. In a Phanerozoic-style plate tectonic setting the implied drift distance is not unlikely but the implied great rapidity of drift is unlike any known Phanerozoic setting. If this interpretation is correct, it has fundamental implications for models of plate movement during the late Archaean. It suggests that at least some late Archaean crust moved thousands of kilometers across the Earth but at a rate incompatible with modern

style plate tectonics. Whereas in Phanerozoic successions flood basalt volcanism is associated with mantle plumes, in the late Archaean, mantle plumes are not necessarily a prerequisite for the formation of flood basalts [*Blake*, 1993]. With a hotter late Archaean mantle, it is conceivable that a different style of tectonism took place.

[71] Finally, it is conceivable that the observed drift is a result of a combination of the above mentioned options. To summarize, the palaeomagnetic shift of 27.2° across the Package 7/8 boundary could be the result of apparent polar wander and indicates a phase of rapid horizontal tectonic movement between circa 2721 Ma and circa 2718 Ma, although other explanations cannot be ruled out. Work in progress, i.e., additional sampling of Packages 7 and 8 at different locations, will aid in further constraining the drift rate.

7.6. Geomagnetic Reversals

[72] The antipodal directions of Package 2 with respect to Package 1 beneath and Package 4 above are interpreted as the record of two geomagnetic reversals, one which occurred between 2772 ± 2 Ma and circa 2766 Ma, and one between circa 2766 Ma and circa 2741 Ma (Figures 3 and 10). Following the Package 2 reversal there is no record of magnetic reversals in the section studied. This interval without geomagnetic reversals has a minimum duration of 26 Myr (from circa 2741 Ma to circa 2715 Ma). While reversals may have occurred during this period and have not been recorded, this period of single polarity is comparable in duration with the Cretaceous Normal Superchron (CNS, circa 30 Myr [*Cande and Kent*, 1995]). A discussion about the occurrence and importance of Superchrons during the Archaean, however, is beyond the scope of this paper.

[73] The oldest Archaean geomagnetic reversal reported to date is from the Kaap Valley pluton of South Africa [*Layer et al.*, 1996]. The authors sampled a variety of rock types of different ages and argued that if all end vectors were plotted together and contoured, a pattern of higher-density distributions of directions was found, but a reversal test was not carried out. The exact age of the Kaap Valley pluton reversal could not be further constrained as being younger than 3224 Ma and older than circa 2000 Ma.

[74] The magnetic reversals in the Nullagine Supersequence are, however, the oldest unambiguous and precisely dated Archaean reversals, and importantly, they are strata-bound and recorded in a single continuous stratigraphic section. This implies that there is no uncertainty about the relative age of the rocks and the normal-reverse-normal sequence. In addition, the data presented here pass the reversal test and the encountered NRM is demonstratively primary. The next younger reported reversal occurs at 2680 ± 10 Ma in the Tanzania Craton [*Meert et al.*, 1994].

[75] It is also likely that a period of reversed polarity occurred between circa 2700 and circa 1700 Myr since the MT directions have all reverse directions. This is consistent with palaeomagnetic data from the circa 2500 Ma Hamersley BIFs [e.g., *Schmidt and Clark*, 1994; *Li et al.*, 2000], which have reverse directions as well.

7.7. Implications for the Vaalbara Hypothesis

[76] Recently, *Cheney* [1996] put forward the hypothesis that between 2.7 and 2.1 Ga the Pilbara and Kaapvaal were part of the same continent, named "Vaalbara." *Zegers et al.* [1998] made a palaeomagnetic reconstruction showing that the Vaalbara supercontinent may have existed between 3.1 and 2.7 Ga. *Wingate* [1998] compared the mean palaeolatitude of 34.3° ± 6.4° from the interpreted 2772 ± 2 Ma Mount Roe basalt (Package 1 is part of the Mount Roe basalt; Figure 4), as published by *Schmidt and Embleton* [1985], with the slightly older palaeolatitude of the 2782 ± 5 Ma (concordant SHRIMP U-Pb, zircon [*Wingate*, 1999]) Derdepoort basalts, Kaapvaal Craton. *Wingate* [1998] found a mean palaeolatitude of 64.5° ± 17.5° (95% confidence limit) for the Derdepoort basalts and concluded that it is unlikely that the Kaapvaal Craton and the Pilbara Craton were part of the same Vaalbara continent at 2.77–2.78 Ga since there is a gap of 6.3° between the minimum palaeolatitude of the Derdepoort basalts and the maximum palaeolatitude of the Mount Roe basalt (Figure 11).

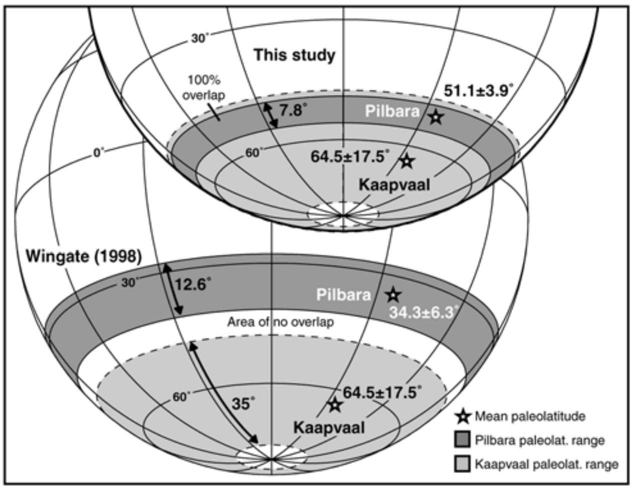

Figure 11. Palaeolatitude reconstructions for the Pilbara and Kaapvaal Cratons at 2.78–2.77 Ga after *Wingate* [1998] (lower globe) compared to this study (upper globe). Reconstructions are based on average palaeolatitudes, which are indicated by stars and the corresponding 95% confidence limits, which are indicated by grey areas). The possible range of Kaapvaal Craton palaeolatitudes in the reconstruction of *Wingate* [1998] compared with the possible range of Pilbara Craton palaeolatitudes from *Schmidt and Embleton* [1985] do not overlap. However, the possible range of Kaapvaal Craton palaeolatitudes does overlap with the possible range of Package 1 palaeolatitudes from this study.

[77] Now, with better constrained data from this study, a similar palaeolatitude reconstruction has been made. With a mean palaeolatitude of 51.1° ± 3.9° for Package 1, the data fall well within the range of 64.5° ± 17.5° for the palaeolatitude of the Derdepoort basalts (Figure 11). Earlier studies of the Black Range and Cajuput Dykes [*Embleton*, 1978] gave palaeolatitudes similar to those found in this study but were not included in the reconstructions of Figure 11. The new data imply that the Vaalbara hypothesis cannot be rejected at 2.78–2.77 Ga; however, since longitude is not constrained in palaeolatitude reconstructions, the Pilbara and Kaapvaal Cratons could still have been situated

up to 180° away from each other. Further, because of a minimum age difference of 3 Myr and an average age difference of 10 Myr between the Kaapvaal and Pilbara basalts, matching palaeolatitudes do not prove the Vaalbara hypothesis at 2.78–2.77 Ga, since this study shows that large amounts of drift may occur within a few million years in the late Archaean. Finally, the errors on the Kaapvaal Craton palaeolatitude determinations are still significant and therefore more sampling is needed. Nevertheless, we conclude that with the data available at this moment, the Vaalbara hypothesis cannot be rejected.

8. Conclusions

[78] This study has demonstrated that a meaningful APWP can be constructed for a late Archaean succession. Importantly, there is no ambiguity about the relative ages of the obtained pole positions since the data come from a single stratigraphic succession. Further, the availability of precise, robust geochronology within the succession enables the determination of absolute ages for the palaeomagnetic poles. The results of this study are summarized as follows:

[79] 1. On the basis of positive field tests and the ability to distinguish between lightning affected directions, overprint directions, and high-temperature directions, we conclude that the high-temperature NRM component is of primary origin, acquired at the time of cooling.

[80] 2. Late Archaean-aged dyke suites can be palaeomagnetically correlated to flood basalt packages, providing additional evidence for comagmatic relationships.

[81] 3. Contrary to the suggestion of *Wingate* [1998], the Vaalbara hypothesis cannot be rejected for the 2.78–2.77 Ga interval since the palaeolatitude of Package 1 lies well within the 95% confidence limits of the palaeolatitude of the Derdepoort basalts.

[82] 4. Within a circa 60 Myr succession, the geomagnetic field has reversed at least twice. It appears that the geomagnetic field in the late Archaean was mostly of single polarity. However, there are significant time intervals that have not been sampled (e.g., Package 3 and most of Package 4, circa 2766–<2752 Ma; Figure 3). These may contain additional geomagnetic field reversals.

[83] 5. It is possible to generate meaningful palaeopole positions for almost all packages within the Nullagine and Mount Jope Supersequences and to construct a consistent APWP.

[84] 6. A major palaeomagnetic break occurs at the Package 7/8 boundary, demonstrating the unconformable nature of this boundary. Assuming that this break reflects plate movement, this result supports the tectonic model for rifting of the Mount Jope Supersequence [*Blake and Barley*, 1992; *Blake*, 1993, 2001]. The results indicate a possible average drift rate as high as 100 cm per year, which is an order of magnitude faster than the modern plate tectonic drift rate.

[85] **Acknowledgments.** This work was conducted under the programme of the Vening Meinesz Research School of Geodynamics (VMSG). We thank Alkane Exploration N. L., in particular D. I. Chalmers (Exploration Manager), for providing logistical support and allowing access to their tenements. Peter Selkin and an anonymous reviewer are thanked for their thorough reviews, which have improved the manuscript. Thanks are also due to Mark Barley, Mark Dekkers, Carmen Gómez Portilla, Dave Heslop, Ton van Hoof, Armelle Kloppenburg, Henk Meijer, Tom Mullender, and Dave "dynamite" Taylor. The Schürmann Fonds is thanked for additional funding for fieldwork, grants 1997, 1999, and 2001/14.

References

Arndt, N. T., D. R. Nelson, W. Compston, A. F. Trendall, and A. M. Thorne, The age of the Fortescue Group, Hamersley basin, Western Australia, from ion microprobe zircon U-Pb results, *Aust. J. Earth Sci.*, *38*, 261–281, 1991.

Barley, M. E., A. L. Pickard, and P. J. Sylvester, Emplacement of a large igneous province as a possible cause of banded iron formation 2.45 billion years ago, *Nature*, *385*, 55–58, 1997.

Blake, T. S., Late Archaean crustal extension, sedimentary basin formation, flood basalt volcanism and continental rifting: The Nullagine and Mount Jope Supersequences, Western Australia, *Precambrian Res.*, *60*, 185–241, 1993.

Blake, T. S., Cyclic continental mafic tuff and flood basalt volcanism in the late Archaean Nullagine and Mount Jope Supersequences in the eastern Pilbara, Western Australia, *Precambrian Res.*, *107*, 139–177, 2001.

Blake, T. S., and M. E. Barley, Tectonic evolution of the late Archean to Early Proterozoic Mount Bruce Megasequence set, Western Australia, *Tectonics*, *11*(6), 1415–1425, 1992.

Blake, T. S., and N. J. McNaughton, A geochronological framework for the Pilbara region, *Publ. Univ. West. Aust. Geol. Dep. Ext. Serv.*, *9*, 1–23, 1984.

Buchan, K. L., J. K. Mortensen, K. D. Card, and J. A. Percival, Paleomagnetism and U-Pb geochronology of diabase dyke swarms of Minto block, Superior Province, Quebec, Canada, *Can. J. Earth Sci.*, *35*(9), 1054–1069, 1998.

Cande, S. C., and D. V. Kent, Revised calibration of the geomagnetic polarity timescale for the Late Cretaceous and Cenozoic, *J. Geophys. Res.*, *100*(B4), 6093–6095, 1995.

Cheney, E. S., Sequence stratigraphy and plate tectonic significance of the Transvaal succession of southern Africa and its equivalent in Western Australia, *Precambrian Res.*, *79*, 3–24, 1996.

Courtillot, V., and J. Besse, Magnetic field reversals, polar wander, and core-mantle coupling, *Science*, *237*, 1140–1147, 1987.

de Wit, M. J., On Archaean granites, greenstones, cratons and tectonics: Does the evidence demand a verdict?, *Precambrian Res.*, *91*, 181–226, 1998.

Embleton, B. J. J., The paleomagnetism of 2400 M.Y. old rocks from the Australian Pilbara Craton and its relation to Archean-Proterozoic tectonics, *Precambrian Res.*, *6*, 275–291, 1978.

Fisher, R. A., Dispersion on a sphere, *Proc. R. Soc. London*, *217*, 295–305, 1953.

Graham, K. W. T., The re-magnetization of a surface outcrop by lightning currents, *Geophys. J. R. Astron. Soc.*, *6*, 85–102, 1961.

Gulson, B. L., and M. J. Korsch, Isotope studies, biennial report 1981/1982, pp. 24–26, Commonwealth Sci. and Ind. Res. Organ. Dev. of Miner. Phys., Sydney, N. S. W., Australia, 1983.

Hallimond, A. F., and E. F. Herroun, Laboratory determinations of the magnetic properties of certain igneous rocks, *Proc. R. Soc. London, Ser. A*, *141*, 302–314, 1933.

Hamilton, W. B., Archean magmatism and deformation were not products of plate tectonics, *Precambrian Res.*, *91*, 143–181, 1998.

Hickman, A. H., and S. L. Lipple, Marble Bar, Western Australia, 1:25,0000, *Geol. Ser Sheet SF50-8*, Geol. Surv. of W. Aust., Perth, 1978.

Idnurm, M., and J. W. Giddings, Australian Precambrian polar wander: A review, *Precambrian Res.*, *40/41*, 61–88, 1988.

Kent, D. V., and M. A. Smethurst, Shallow bias of paleomagnetic inclinations in the Paleozoic and Precambrian, *Earth Planet. Sci. Lett.*, *160*, 391–402, 1998.

Kirschvink, J. L., The least-squares line and plane and the analysis of palaeomagnetic data, *Geophys. J. R. Astron. Soc.*, *62*, 699–718, 1980.

Kirschvink, J. L., R. L. Ripperdan, and D. A. Evans, Evidence for a large-scale reorganisation of Early Cambrian continental landmasses by inertial interchange true polar wander, *Science*, *277*, 541–545, 1997.

Layer, P. W., A. Kröner, and M. McWilliams, An Archean geomagnetic reversal in the Kaap Valley pluton, South Africa, *Science*, *273*, 943–946, 1996.

Li, Z. X., W. Guo, and C. M. Powell, Timing and genesis of Hamersley BIF-hosted iron ore deposits: A new palaeomagnetic interpretation, 216 pp., *MERIWA 199*, Miner. and Energy Res. Inst. of West. Aust., Perth, West. Aust., Australia, 2000.

MacLeod, W. N., L. E. de la Hunty, W. R. Jones, and R. Halligan, A preliminary report on the Hamersley Iron Province, North-west Division, *Annu. Rep. Geol. Surv. West. Aust.*, *1962*, 44–54, 1963.

Marsh, J. S., P. R. Hooper, J. Rehacek, R. A. Duncan, and A. R. Duncan, Stratigraphy and age of Karoo basalts of Lesotho and implications for correlations with the Karoo igneous province, in *Large Igneous Provinces*: *Continental, Oceanic, and Planetary Flood Volcanism*, *Geophys. Mongr. Ser.*, vol. 100, edited by J. J. Mahoney and M. F. Coffin, pp. 247–272, AGU, Washington, D. C., 1997.

McElhinny, M. W., and J. Lock, IAGA paleomagnetic databases with Access, *Surv. Geophys.*, *17*, 575–591, 1996.

McElhinny, M. W., and P. L. McFadden, *Paleomagnetism*; *continents and oceans*, *Int. Geophys. Ser.*, vol. 73, 386 pp., Academic, San Diego, Calif., 2000.

McFadden, P. L., A new fold test for palaeomagnetic studies, *Geophys. J. Int.*, *103*, 163–169, 1990.

McFadden, P. L., and M. W. McElhinny, Classification of the reversal test in palaeomagnetism, *Geophys. J. Int.*, *103*, 725–729, 1990.

McFadden, P. L., and M. C. McElhinny, Combining groups of paeomagnetic directions or poles, *Geophys. Res. Lett.*, *22*, 2191–2194, 1995.

Meert, G. M., A paleomagnetic analysis of Cambrian true polar wander, *Earth Planet. Sci. Lett.*, *168*, 131–144, 1999.

Meert, G. M., R. van der Voo, C. M. Powell, Z. X. Li, M. C. McElhinny, Z. Chen, and D. T. A. Symons, A plate-tectonic speed limit?, *Nature*, *363*, 216–217, 1993.

Meert, G. M., R. van der Voo, and J. Patel, Paleomagnetism of the late Archean Nyanzian System, western Kenya, *Precambrian Res.*, *69*, 113–131, 1994.

Morimoto, C., O. Otofuji, M. Miki, H. Tanaka, and T. Itaya, Preliminary paleomagnetic results of an Archean dolerite dyke of west Greenland: Geomagnetic field intensity at 2.8 Ga, *Geophys. J. Int.*, *128*, 585–593, 1997.

Nelson, D. R., Compilation of SHRIMP U-Pb zircon geochronology data, 1998, Geol. Surv. of W. Australia, Perth, 1999.

Nelson, D. R., A. F. Trendall, J. R. de Laeter, N. J. Grobler, and I. R. Fletcher, A comparative study of the geochemical and isotopic systematics of late Archean flood basalts from the Pilbara and Kaapvaal Cratons, *Precambrian Res.*, *54*, 231–256, 1992.

Pidgeon, R. T., Geochronological constraints on early volcanic evolution of the Pilbara Block, Western Australia, *Aust. J. Earth Sci.*, *31*, 237–242, 1984.

Pollack, H. N., Thermal characteristics of the Archean, in *Greenstone Belts*, edited by M. J. de Wit and L. D. Ashwal, pp. 223–233, Oxford Univ. Press, New York, 1997.

Reidel, S. P., and P. R. Hooper, Volcanism and tectonism in the Columbia river flood-basalt province, *Spec. Pap. Geol. Soc. Am.*, *239*, 386 pp., 1989.

Saunders, A. D., J. G. Fitton, A. C. Kerr, M. J. Norry, and R. W. Kent, The North Atlantic igneous province, in *Large Igneous Provinces*: *Continental, Oceanic, and Planetary Flood Volcanism*, *Geophys. Mongr. Ser.*, vol. 100, edited by J. J. Mahoney and M. F. Coffin, pp. 45–93, AGU, Washington, D. C., 1997.

Schmidt, P. W., and D. A. Clark, Paleomagnetism and magnetic anisotropy of Proterozoic banded iron formations and iron ores of the Hamersley Basin, Western Australia, *Precambrian Res.*, *69*, 133–155, 1994.

Schmidt, P. W., and J. J. Embleton, Prefolding and overprint magnetic signatures in Precambrian (~2.9–2.7 Ga) igneous rocks from the Pilbara Craton and Hamersley Basin, NW Australia, *J. Geophys. Res.*, *90*(B4), 2967–2984, 1985.

Shipunov, S. V., A. A. Muraviev, and M. L. Bazhenov, A new conglomerate test in palaeomagnetism, *Geophys. J. Int.*, *133*, 721–725, 1998.

Smith, R. E., J. L. Perdrix, and T. C. Parks, Burial metamorphism in the Hamersley Basin, Western Australia, *J. Petrol.*, *23*, 75–102, 1982.

Sumita, I., T. Hatakeyama, A. Yoshira, and Y. Hamano, Paleomagnetism of late Archean rocks of Hamersley Basin, Western Australia and the paleointensity at Early Proterozoic, *Phys. Earth Planet. Inter.*, *128*, 223–241, 2001.

Tauxe, L., and G. S. Watson, The fold test: An eigen analysis approach, *Earth Planet. Sci. Lett.*, *122*, 331–341, 1994.

Thom, R., A. H. Hickman, and R. J. Chin, Nullagine, Western Australia, 1:25,0000, *Geol. Ser. Sheet SF 51-5*, Geol. Surv. of W. Aust., Perth, 1979.

Thorne, A. M., and A. F. Trendall, Geology of the Fortescue Group, Pilbara Craton, Western Australia, *Geol. Surv. West. Aust. Bull.*, 144, 249 pp., 2001.

Thorne, A. M., and I. M. Tyler, Roy Hill, Western Australia, 1:250 000, *Geol. Ser. Sheet SF 50-12*, Geol. Serv. W. Aust., Perth, 1996.

Trendall, A. F., A revision of the Mount Bruce Supergroup, *Annu. Rep. Geol. Surv. West Aust.*, *1978*, 63–71, 1979.

Trendall, A. F., The Hamersley Basin, in *Iron-Formation*: *Facts and Problems*, edited by A. F. Trendall and R. C. Morris, pp. 69–129, Elsevier Sci., New York, 1983.

van der Voo, R., Phanerozoic paleomagnetic poles from Europe and North America and comparisons with continental reconstructions, *Rev. Geophys.*, *28*, 167–206, 1990.

van der Voo, R., and T. H. Torsvik, Evidence for late Paleozoic and Mesozoic non-dipole fields provides an explanation for the Pangea recontruction problems, *Earth Planet. Sci. Lett.*, *187*, 71–81, 2001.

Watson, G. S., A test for randomness of distributions, *Mon. Not. R. Astron. Soc. Geophys. Suppl.*, *7*, 160–161, 1956.

Westphal, M., E. L. Gurevitch, B. V. Samsonov, H. Feinberg, and J. P. Pozzi, Magnetostratigraphy of the lower Triassic volcanics from deep drill SG6 in western Siberia: Evidence for long-lasting Permo-Trassic volcanic activity, *Geophys. J. Int.*, *134*, 254–266, 1998.

Wingate, M. T. D., A palaeomagnetic test of the Kaapvaal-Pilbara (Vaalbara) connection at 2.78 Ga, *S. Afr. J. Geol.*, *101*(4), 257–274, 1998.

Wingate, M. T. D., Ion microprobe baddeleyite and zircon ages for late Archaean mafic dykes of the Pilbara Craton, Western Australia, *Aust. J. Earth Sci.*, *46*, 493–500, 1999.

Zegers, T. E., M. J. de Wit, J. Dann, and S. H. White, Vaalbara, Earth's oldest supercontinent: A combined structural, geochronologic, and paleomagnetic test, *Terra Nova*, *10*(5), 250–259, 1998.

Zhai, Y. J., H. C. Halls, and M. P. Bates, Multiple episodes of dike emplacement along the northwestern margin of the Superior Province, Manitoba, *J. Geophys. Res.*, *99*(B11), 21,717–21,732, 1994.

Zijderveld, J. D. A., Demagnetization in rocks: Analysis of results, in *Methods in Palaeomagnetism*, edited by D. C. Collinson, K. M. Creer, and S. K. Runcorn, pp. 254–286, Elsevier Sci., New York, 1967.

T. S. Blake, 86 Reservoir Street, Chidlow, WA 6556, Australia.

C. G. Langereis, G. Strik, and T. E. Zegers, Palaeomagnetic Laboratory Fort Hoofddijk, Department of Earth Sciences, Utrecht University, Budapestlaan 17, NL-3584 CD Utrecht, Netherlands. (strik@geo.uu.nl)

S. H. White, Department of Earth Sciences, Utrecht University, Budapestlaan 4, NL-3584 CD Utrecht, Netherlands.